University of New Hampshire
University of New Hampshire Scholars' Repository

Master's Theses and Capstones | Student Scholarship

Fall 2012

# Object-based image analysis for forest-type mapping in New Hampshire

Christina Czarnecki
*University of New Hampshire, Durham*

Follow this and additional works at: https://scholars.unh.edu/thesis

Recommended Citation
Czarnecki, Christina, "Object-based image analysis for forest-type mapping in New Hampshire" (2012). *Master's Theses and Capstones*. 741.
https://scholars.unh.edu/thesis/741

This Thesis is brought to you for free and open access by the Student Scholarship at University of New Hampshire Scholars' Repository. It has been accepted for inclusion in Master's Theses and Capstones by an authorized administrator of University of New Hampshire Scholars' Repository. For more information, please contact nicole.hentz@unh.edu.

# OBJECT-BASED IMAGE ANALYSIS FOR FOREST-TYPE MAPPING IN NEW HAMPSHIRE

by

Christina Czarnecki
B.S., Philadelphia University, 2004

THESIS

Submitted to the University of New Hampshire
in Partial Fulfillment of
the Requirements for the Degree of

Masters of Science
in
Natural Resources

September 2012

UMI Number: 1521564

All rights reserved

INFORMATION TO ALL USERS
The quality of this reproduction is dependent upon the quality of the copy submitted.

In the unlikely event that the author did not send a complete manuscript
and there are missing pages, these will be noted. Also, if material had to be removed,
a note will indicate the deletion.

UMI®
Dissertation Publishing

UMI 1521564
Published by ProQuest LLC 2012. Copyright in the Dissertation held by the Author.
Microform Edition © ProQuest LLC.
All rights reserved. This work is protected against
unauthorized copying under Title 17, United States Code.

ProQuest®

ProQuest LLC
789 East Eisenhower Parkway
P.O. Box 1346
Ann Arbor, MI 48106-1346

All rights reserved.
©2012
Christina Czarnecki

**This thesis has been examined and approved.**

Thesis Director, Dr. Russell G. Congalton,
Professor of Remote Sensing and
Geographic Information Systems

Dr. Mark Ducey, Professor
Department of Natural Resources
and the Environment

Lucie Lepine, Research Scientist,
Earth Systems Research Center,
University of New Hampshire

8/8/12
Date

## ACKNOWLEDGEMENTS

Funding was provided by a McIntire-Stennis Research Assistantship (MS-33) (Congalton) offered by the University of New Hampshire Agriculture Experiment Station.

# TABLE OF CONTENTS

## LIST OF TABLES

## LIST OF FIGURES

# ABSTRACT

OBJECT-BASED IMAGE ANALYSIS FOR FOREST-TYPE MAPPING

IN NEW HAMPSHIRE

By

Christina Czarnecki

University of New Hampshire, September 2012

The use of satellite imagery to classify New England forests is inherently complicated due to high species diversity and complex spatial distributions across a landscape. The use of imagery with high spatial resolutions to classify forests has become more commonplace as new satellite technology become available. Pixel-based methods of classification have been traditionally used to identify forest cover types. However, object-based image analysis (OBIA) has been shown to provide more accurate results. This study explored the ability of OBIA to classify forest stands in New Hampshire using two methods: by identifying stands within an IKONOS satellite image, and by identifying individual trees and building them into forest stands.

Forest stands were classified in the IKONOS image using OBIA. However, the spatial resolution was not high enough to distinguish individual tree crowns and therefore, individual trees could not be accurately identified to create forest stands. In addition, the accuracy of labeling forest stands using the OBIA approach was low. In the future, these results could be improved by using a modified classification approach and appropriate sampling scheme more reflective of object-based analysis.

# INTRODUCTION

Remotely-sensed imagery from earth-observing satellites is commonly used in forest management to monitor or quantify land resources. Along with field-based measurements, satellite imagery is used extensively to monitor land cover characteristics such as land cover types (forest, agriculture, urban, water, etc.) over a range of spatial and temporal scales (Dean and Smith, 2003; Carleer and Wolff, 2006; Ekercin, 2007; Hansen et al., 2008; Larrañaga et al., 2011; Van Delm and Gulinck, 2011). By using remotely sensed imagery along with ground reference data, land managers are able to map their resources without having to make field measurements at all of their managed areas. This technique of using imagery to map land cover increases efficiency and reduces the need to visit areas that are difficult or impossible to access. Maps derived from satellite imagery are known as thematic maps. Land cover maps are thematic maps that represent the ground, such as forest, pasture, water, or development. These land cover maps are useful in numerous natural resource applications to describe the spatial distribution and pattern of the land cover characteristics that they represent.

The ability to make accurate maps from remotely sensed data depends in part on the spatial resolution of the imagery. Spatial resolution is the surface area on the ground detected by the sensor, and is described as a pixel (Jensen, 2005). Pixel-based image classification has traditionally been the most common method to classify satellite imagery (Doraiswamy et al., 2004; Paul et al., 2004; Becker et al.,

2007; Röder et al., 2008). Based on pre-determined rules, pixel-based classification categorizes all pixels in an image into a land cover category or theme that best describes them. The result is a thematic map that represents the different land cover types present on the image.

Over the last decade, the amount of high-resolution imagery available for analysis has greatly expanded sensor technology has progressed. Landsat TM, Landsat ETM+, and SPOT imagery, once considered to have high spatial resolutions, are now considered to have moderate resolutions at best because new even higher resolution data sensors have been introduced. Imagery from sensors like Quickbird and IKONOS is widely available and is being used for landscape analysis. Quickbird is a commercial satellite that offers 61cm panchromatic spatial resolution at nadir (the point on the ground directly below the sensor) and 2.4m multispectral spatial resolution at nadir. IKONOS (GeoEye, formally Space Imaging) is a commercial satellite that offers 80cm spatial resolution at nadir for the panchromatic band and 4m spatial resolution at nadir for the multispectral bands. Pixel-based classification is not as accurate when creating thematic maps from imagery with high spatial resolution as it is with moderate spatial resolution data (Blaschke and Strobl, 2001). This can be due to the effects of shadow or single ground objects fractured into many pixels (Townshend et al., 2000; Blaschke and Strobl, 2001).

An alternative to pixel-based classification is object-based image analysis (OBIA), a type of image processing and classification that has provided better results when using high resolution imagery. OBIA uses groups of pixels that represent a homogeneous area in a particular classification category. By averaging or grouping

like-pixels together, statistical separation can be achieved, thereby circumventing many of the problems faced when using pixel-based classifications with high-resolution imagery. Homogeneous landscapes are defined as land that is similar in composition or uniform in its patterns. Examples of similarly composed landscapes include single-species forests and large bodies of water. Uniform patterns include landscapes such as Christmas tree farms or crop fields, where trees or crops are not the only item on the landscape, but are dominant and appear equally spaced. In contrast, heterogeneous landscapes have no discernible pattern and are comprised of multiple features.

In general, more accurate land cover maps are created when classifying high resolution imagery with object-based techniques rather than pixel-based techniques (Desclée et al., 2006; Yan et al., 2006; Cleve et al., 2008; Myint et al., 2011). However, the ability of object-based classification methods to accurately identify individual trees in a forest, and also to identify individual trees by species, is an ongoing topic of research. In the past, New Hampshire forests have been classified using a system based on a classification scheme designed by the Society of American Foresters' (SAF). This classification scheme, first described by Eyre (1980), relies heavily on understory vegetation and ecological relationships to classify forest stands. This may not be conducive to creating accurate forest land cover maps based on satellite imagery. Therefore, the objectives of this study are:

## Objectives

1. Evaluate OBIA as a means to identify individual tree crowns in a high-resolution forested image of New Hampshire, and merge these tree crowns to build forest stands
2. Evaluate OBIA as a means to create forest stand maps using the New Hampshire SAF classification system

# CHAPTER I

# LITERATURE REVIEW

The literature review is divided into six sections. The first section describes the fundamentals of satellite imagery and the basic types of image classifications. The second section compares two types of image classification techniques as they pertain to different types of satellite imagery. The third section describes the steps to gathering necessary field data to aid in image classification and creation of a classification protocol. Next, pre-processing of satellite imagery for classification is discussed. Then, the steps to OBIA are explained for creating thematic maps of forest cover types. Finally, an overview of the accuracy of thematic maps is explored.

## Background

Satellite-based sensors record radiance that reaches the sensor from the ground and atmosphere. Radiance is defined as the intensity of reflected light.

Sensors can be thought of as dividing the EM spectrum into one or more "bands" that measure radiance within a defined portion of the spectrum. A sensor can have several bands that measure radiance within different parts of the EM spectrum (Campbell and Wynne, 2011). The bands may be continuous or discrete, and wide or narrow. These characteristics refer to the *spectral resolution* of a satellite's sensor.

Areas on the ground are represented in a satellite image by pixels, which are organized into rows and columns. Each pixel's numerical value refers to the radiance within that particular band. Low pixel values indicate high absorption of light, while high pixel values indicate high levels of light reflection. The ability of the sensor to distinguish slight differences in light intensity refers to its *radiometric resolution*, which is measured in bits. Jensen (2005) defines radiometric resolution as the sensitivity of the satellite sensor to detect differences in signal strength as it records the radiant flux reflected, emitted, or back-scattered from the terrain. Radiometric resolution is quantified as the levels of gray on an image. An 8-bit image will have up to 256 different pixel values, or 256 levels of gray. An 11-bit image that measures the same radiance as the 8-bit image will be able to measure up to 2,048 different pixel values, thereby capturing more detail or subtleties within the radiance than would the 8-bit image. Jensen (2005) likens radiometric resolution to a ruler—if precision measurements are needed, a ruler with over 2,000 levels of gray is better than one with 256 levels of gray.

Individual pixels also represent a geographic area. The area of each pixel refers to the image's *spatial resolution*. The spatial resolution can be considered

coarse when it covers a large area (e.g., $1km^2$ or greater), or fine when it covers a small area (e.g., $60cm^2$).

Pixel-based image classification has traditionally been the most common method to classify satellite imagery (Dean and Smith, 2003; Jobin et al., 2008), where each pixel discretely categorized based on its spectral value. These categories are set by the producer (the person performing the classification), and classification is facilitated using a supervised approach, an unsupervised approach, or a combination of the two (Jensen, 2005). In a supervised classification, the producer chooses training areas (defined homogeneous areas) that are representative of a classification category. The spectral signatures of each training area are analyzed, and then all other pixels are classified based on those signatures. Supervised classification is best used when the categories of interest are easily defined and spectrally separable, the area of interest is relatively small, and the producer has *in situ* knowledge of the area. Unlike supervised classification, there are no training areas involved in unsupervised classification. Pixels in an image are separated into classes using a pre-defined number of categories and a confidence threshold. Once the pixels are divided into clusters, the producer then labels each class. Unsupervised classifications are best used when trying to classify relatively large areas on the ground, and for areas where there is little or no *in situ* knowledge (Jensen, 2005; Campbell and Wynne, 2011).

Recently, the high volumes of imagery available to land and resource managers—more specifically, the advent of multiple sources of readily available, high spatial resolution imagery—have made it necessary to take a different

approach to image classification. The large amount of data can become overwhelming due to large file sizes, temporal abundance and variability, differing spatial and spectral scales, and the time-intensive methods used to interpret the data.

## Land Cover Mapping: Pixels vs. Objects

The increase in spatial resolution means increased variability within areas that may have otherwise been defined as homogeneous. For example, on a spatially coarse image, a pixel might average the spectral reflectance of a group of oak trees. Another pixel might represent a wetland. As the spatial resolution becomes more refined, the group of trees becomes one tree, or only a part of tree. The wetland pixel is now several pixels that represent varying degrees of wetness within the wetland. A higher spatial resolution increases the spectral variability within the trees or wetland, and therefore can decrease the statistical separation between each pixel. These increases in spectral variability makes separability using pixel-based classification methods more difficult (Carleer et al., 2004).

The grouping of pixels in an image into objects, or segments, is called segmentation. Segmentation goes by several names in the literature, including segmentation, segment-based classification, object-based classification, region-based classification, and object-based image analysis (OBIA); objects can also be referred to as segments or polygons. Object-based image classification is an effective alternative to a pixel-based approach. A substantial difference between traditional pixel-based image classification and object-based classification is that

pixel-based classification does not use any spatial concepts (Blaschke and Strobl, 2001); classification is based on the spectral signature of a single pixel without consideration of other pixels around it. However, increases in spatial resolution increases the probability that pixels surrounding the pixel of interest are the same (Blaschke and Hay, 2001). As a result, the signal a pixel radiates as a representative of a particular class becomes contaminated by the signals of the pixels around it (Townshend et al., 2000). With an increase in spatial resolution comes a loss in statistical separability within the spectral data space, thereby reducing the accuracy of pixel-based classifications (Carleer et al., 2005).

The term "land cover" is used to describe different types of land. Common categories include forest, water, urban, and agriculture. This is different from "land use", which categorizes land based on its most common use. For example, while 'urban' describes a land cover type, 'residential', 'commercial', 'industrial', and 'transportation' are land use types. In the past, common types of imagery used to classify land cover included Landsat MSS, Landsat TM, MODIS, AVHRR, and others. The spatial resolutions of Landsat MSS and TM data are approximately 60m and 30m in the reflectance bands, respectively (Chander et al., 2009). MODIS products range from 250m – 1000m in spatial resolution depending on the product (LPDAAC, 2011). In traditional pixel-based classification, the spectral signal of each pixel across multiple bands of the electromagnetic spectrum is analyzed for characteristics that separate it from different pixels on the same image. A single pixel represents a spectral aggregation of all land cover types within its boundaries. One or more land cover types would be represented within a single pixel.

However, improvements in sensor technology allow for imagery with much higher spatial resolutions (Table 1). With this increase in spatial resolution comes a lower spectral resolution and a higher within-class spectral variability, thereby decreasing the statistical separability of spectral information into land cover classes. The biggest cause of increased internal variability within classes is pixels composed of shadow (Carleer et al., 2005). Another culprit that decreases separability is spatial autocorrelation, defined as the degree of dependency among observations in a geographic space; the signal of an individual pixel is highly influenced by the pixels around it (Townshend et al., 2000).

Object-based classification attempts to identify patterns in an image and use contextual information to group pixels into clusters that represent the same object. By grouping pixels into meaningful objects, spectral variability within a segment is minimized and differences between segments are maximized (Flanders et al., 2003). An object-based approach also reduces the effects of spatial autocorrelation. In general, high-resolution imagery is classified more accurately when using object-based classifications than pixel-based classifications (Townshend et al., 2000; Blaschke and Strobl, 2001; Coe et al., 2005).

Table 1: Minimum and maximum spatial resolutions for selected optical satellite sensors

| Sensor | Spatial Resolution | | Spectral Resolution | |
|---|---|---|---|---|
| | Minimum | Maximum | Minimum | Maximum |
| MODIS | 250m | 1km | 405nm | 14.39μm |
| Landsat TM | 30m | -- | 450nm | 2350nm |
| ASTER | 15m | 30m | 520nm | 2430nm |
| RapidEye | 5m | 5m | 440nm | 850nm |
| SPOT-5 | 2.5m | 20m | 480nm | 1750nm |
| ALOS | 2.5m | 10m | 420nm | 890nm |
| SPOT-6, SPOT-7 | 1.5m | 6m | 450nm | 890nm |
| IKONOS | 0.82m | 3.2m | 445nm | 929nm |
| QuickBird, WorldView-1, WorldView-2 | 0.5m | 2.62m | 400nm | 1040nm |
| Geoeye-1 | 0.41m | 1.65m | 450nm | 920nm |

## Sampling Design and Data Collection

A thematic map cannot be created without first devising a classification system. A good classification system starts with broad or generalized classes that allow for subdivisions into more specific classes; subdivision continues until a predefined, minimum-sized area is reached (Husch, 1971). As these classes become more specific, the overlap in characteristics between classes lessens until mutually exclusive classes are developed. There are four main rules used when devising a classification scheme--that classes within the scheme be hierarchical in nature, devised of labels and rules, totally exhaustive, and mutually exclusive (Congalton and Green, 2009). A hierarchical classification scheme is synonymous to dichotomous key, where specific classes fall iteratively under more general descriptions. Each class should be clearly labeled and refer to its corresponding description. Also, each class description must adhere to a set of rules or definitions

that allow for a systematic and consistent classification. A totally exhaustive classification scheme ensures that every area on the map falls into a class, and that no area is left unclassified. Finally, a mutually exclusive set of classes ensures that each mapped area can only fall into one class. However, this final rule of sample exclusivity conflicts with the principles of fuzzy classifications, which is discussed in more detail in the next section.

For a forest classification system, a forest as a whole would be the most general class and be at the top of the class hierarchy. According to Husch (1971), there are three characteristics of a forest that can be used to devise a forest classification system: size, site, and composition. A system based on size creates a class hierarchy based on such factors as tree height, basal area, or stand density (a forest stand is comprised of several trees grouped together). A system based on site would focus on qualities such as soil or terrain characteristics, or the general purpose or use of the land. A system based on composition is the most widely used type of classification and focuses on species-specific characterizations (Husch, 1971).

The composition-based classification system used for this study was based on rules and definitions set forth by the Society of American Foresters (SAF), which states that the dominant cover must be of trees, and must cover at least 25% of the area (see 'Table 2' for descriptions). Definitions of forest cover types are named after the predominant tree species, which is determined by basal area. The SAF defines a *pure* forest stand as stocked by 80% or more of a single species. A *majority* is comprised of a single species representing greater than 50% of a forest stand. A

*plurality* involves a single species that comprises the largest proportion in mixed stands.

Forest classifications inherently include rules for categorizing forest species into stands and/or rules for sampling forests to determine stand types. Historically, sampling units have been categorized as either points or areal units. The term "point" is used to represent a correspondence between the resulting classification on the thematic map and its associated area on the earth. Areal units are defined by a spatial extent, such as a pixel, a polygon, or a unit of measurement (hectare, acre, square meter, etc.). It should be noted that although single pixels have been used as sampling units, they are often ineffective as such and instead should be used in clusters of pixels or another unit of measurement mentioned above (Congalton and Green, 1999, 2009).

Stehman and Czaplewski (1998) released an overview of recommended sampling units using over thirty published works. Very few of these reviewed publications agree on a single "proper" sampling unit; however, it is agreed that a sampling unit must be optimized for its relevant application. The USDA Forest Service has used both points and areal units for its Forest Inventory and Analysis National Program (Birdsey and Schreuder, 1992). This program began in 1930 with systematic surveys of all forests by using areal extents. This technique was later changed to point-based sampling, where the points represent designated areas on the ground (ex. 20x20 plot). This was deemed more efficient and could be aided with the use of aerial photography. The USGS released a combined land use/ land cover classification scheme in an attempt to create a standardized system that could

be utilized by both private and government agencies (Anderson et al., 1976). The classification scheme uses only satellite imagery or aerial photography as its reference for classification, and is hierarchical based on the spatial scale of imagery or photos used.

Table 2: Description of fine-scale subclasses for forest cover classification based on SAF definitions

| Title | Code | Description |
|---|---|---|
| White Pine | WP | Eastern white pine (*Pinus strobus*) comprises 70% or more of the stand |
| Hemlock | HE | Eastern hemlock (*Tsuga canadensis*) comprises 70% or more of the stand |
| Pine/ Hemlock | WH | Eastern white pine and eastern hemlock together comprise a majority of the stand, and each represent at least 25% of the total. Neither species alone comprises more than 50% of the total |
| Beech | BH | American beech (*Fagus grandifolia*) comprises at least 30% of the forest cover type. Eastern white pine and/or eastern hemlock comprise less than 50% of the forest cover type |
| Red Maple | RM | Red maple (*Acer rubrum*), sugar maple (*Acer saccharum*), or some combination of the two, represent 50% or more of the forest stand |
| Oak | OAK | White oak (*Quercus alba*), black oak (*Quercus velutina*), and/or northern red oak (*Quercus rubra*) comprise at least 50% of the stocking. Eastern white pine and/or eastern hemlock comprise less than 50% of the forest cover type |
| Mixed | MX | At least two or more deciduous species combined (besides *Quercus spp.*) represent 30% or more of the forested area |
| Other | OF | Any mix of coniferous and/or deciduous species not represented in one of the above categories |
| Non-forested | NF | Any other vegetated cover type (forest within permanent or semi-permanent standing water, agriculture, pasture, shrubland, etc) |

Data collection for image classification consists of two separate datasets: training datasets and reference datasets. The method used to collect data depends on several factors, including the minimum mapping unit (MMU, the minimum size for feature to be mapped), classification type (pixel or polygon), number of classes in the class hierarchy, and distribution of said classes on the image. Probability sampling is recommended for image classification because it takes into account the probability of a sampling unit being chosen for training or accuracy assessment, and thereby accounting for the percentage of that class that's present in the image (Congalton, 1991; Stehman and Czaplewski, 1998; Congalton and Green, 2009). There are several options for choosing a sampling scheme that include random, systematic, or stratified sampling schemes. Stratified random sampling is the most common sampling scheme used for image classification because it avoids spatial biases while ensuring that samples are collected for each of the classes, or strata, in the classification scheme (Stehman and Czaplewski, 1998; Congalton and Green, 1999; Radoux et al., 2011).

Reference samples and training samples should be chosen without replacement to ensure that the same sample isn't used for both classification training and accuracy assessment, thereby making accuracy assessment less efficient. Reference samples can be created by photo interpretation when possible and by field collection when photo interpretation is not possible. However, ground sample collection can be limited by such factors as time, money, and area inaccessibility. Consequently, a minimum number of reference samples per class should be calculated ahead of time to ensure the statistical reliability of an accuracy

assessment. Collection of reference samples and training samples can be completed concurrently or separately. Congalton and Green (1999) recommend collecting 50 samples per class for areas totaling less than 1 million acres and with fewer than 12 classes as a "rule of thumb".

## Data Preprocessing

Steps can be taken prior to image classification to enhance the satellite imagery. This preparation can yield new data layers for use with the original spectral bands, or can correct existing bands for errors due to geometry (errors in pixel location) or atmospheric interference (spectral differences due to aerosol particles).

The creation of vegetation indices is a useful tool for extracting information in a pixel specific to vegetation health, phenology, or influences due to sun angle or sensor viewing angle. A vegetation index uses two or more image bands and performs one or more mathematic operations the pixel's spectra. Vegetation indices can serve as a means to normalize data, differentiate vegetation from other surfaces that reflect light in the near-infrared, and emphasize particular spectral features that may otherwise be difficult to discern such as vegetation health. Some of the most common vegetation indices are a simple ratio (SR) , the normalized difference vegetation index (NDVI), and the enhanced vegetation index (EVI) (Jensen, 2005),

$$SR = \frac{\rho_{nir}}{\rho_{red}} \tag{1}$$

where: SR = the ratio of reflected radiance from the red & infrared spectrum
$\rho_{nir}$ = the reflected radiance within the near infrared spectrum
$\rho_{red}$ = the reflected radiance within the visible red spectrum

$$NDVI = \frac{(\rho_{nir} - \rho_{red})}{(\rho_{nir} + \rho_{red})} \tag{2}$$

where: NDVI = the normalized difference vegetation index
$\rho_{nir}$ = the band within the near infrared spectrum
$\rho_{red}$ = the band within the visible red spectrum

$$EVI = G * \frac{(\rho_{nir} - \rho_{red})}{(\rho_{nir} + C_1 * \rho_{red} - C_2 * \rho_{blue} + L)} * (1 + L) \tag{3}$$

where: EVI = the enhanced vegetation index
$\rho_{nir}$ = the band within the near infrared spectrum
$\rho_{red}$ = the band within the visible red spectrum
G = gain coefficient
$C_1$, $C_2$ = aerosol coefficients
$L$ = adjusts for effects from background

There are many other types of vegetation indices, but their utility is limited by the spectral extent and resolution of the sensor.

An important preprocessing step is to ensure that atmospheric interference due to clouds, water vapor, or aerosols are corrected. If left unaddressed, these interferences can limit spectral data interpretation. There are several different approaches to correcting an image for atmospheric interferences. One method, called Top-Of-Atmosphere (TOA) corrections, uses parameters obtained from the satellite's sensors (e.g. gain coefficients) as well as orbit data (e.g. time of year or sun angle) to correct pixel values (see 'Data Preprocessing', pg. 34) for correction.

Principal components analysis (PCA) can also be performed on multi-band imagery to reduce its dimensionality to only the most important information. Since the bands within a multispectral image are highly correlated, performing a PCA decorrelates the information by performing a transformation within the data's feature space and creating new "bands" that account for most of the variability in the original data. .

## Segmentation

The human brain has the ability to recognize objects and perceive patterns, and naturally uses contextual information to understand what it's seeing; it naturally segments what it's seeing into meaningful objects. Object-based classification attempts to replicate this process of recognition to overcome the limitations of pixel-based classification. Segmentation and classification of natural landscapes such as forested images must adhere to the basic principles of landscape ecology and attempt to capture the relationships between spatial patterns and related ecological processes (Farina, 2000; Turner et al., 2001; Burnett and Blaschke, 2003). A landscape can be defined as a continuous spatial extent made up of a configuration of discrete patches in which ecological processes take place at different spatial and temporal scales (Farina, 2000). Scale is the spatial and temporal limit defined by the observer, and there are multiple scales within a landscape depending on perception or a given ecological process (Allen and Starr, 1988; Farina, 2000). The view that a landscape is neither a level of spatial resolution nor a level of organization was a theory that was believed at the advent of

the study of landscape ecology, and on the whole has been abandoned in light of hierarchy theory (Allen and Starr, 1988; Wu, 1999; Farina, 2000; Blaschke and Lang, 2006; Farina, 2006). Hierarchy theory describes different spatio-temporal scales across a landscape.

Segmentation of a forested image requires breaking down a landscape (a continuous spatial extent) into discrete subsystems for the purposes of classification. To achieve successful image classification, a segmentation algorithm must be chosen based on factors such as data types or intended use of the final product (Baatz and Schäpe, 2000; Philipp-Foliguet and Guigues, 2008). One such algorithm is the *fractal net evolution approach* (FNEA). FNEA is a multi-resolution or multi-scale approach, meaning that it operates on many different scales at once, and can be directly related to the way an ecologist might segment a landscape. Just as principles of landscape ecology and hierarchy theory use patches to divide a continuous landscape into discrete units, segments that are created from pixels in an image can be thought of as discrete patches. The size of the patch depends on the scale of interest. FNEA handles this ecological hierarchy by creating smaller patches—smaller groups of pixels—and nesting them into bigger patches to create multiple levels. This makes FNEA an appropriate algorithm for image segmentation of a natural landscape. However, one problem when attempting to divide a landscape continuum into discrete patches is the subjectivity of the divider; there are many ways that a continuous landscape can be divided (Burnett and Blaschke, 2003).

FNEA segments an image by identifying discontinuities between pixels (Blaschke and Strobl, 2001). FNEA accounts for the representation of several scale domains in one image, and uses a region-merging technique starting with single-pixel objects. In numerous subsequent steps, smaller image objects composed of several pixels are merged into bigger objects. FNEA creates segments that follow a *homogeneity criterion*, in which "the average heterogeneity of pixels [is] minimized. Each pixel is weighted with the heterogeneity of the image object to which it belongs" (Baatz and Schäpe, 2000). The goal is to increase between-object variability and decrease within-object variability (Flanders et al., 2003). The collective result is multi-resolution segmentation, which captures objects on the image at multiple scales. This multi-scale technique is used to construct a hierarchical network of image objects. This network is topologically definite, meaning that all hierarchical levels are created by breaking segments down into sub-objects or grouping segments together into super-objects. Under-segmentation (multiple objects joined by one set of boundaries) and over-segmentation (a single object identified by multiple sets of boundaries) should be avoided (Carleer and Wolff, 2006).

When defining the parameters for image segmentation using FNEA, three homogeneity criteria are considered: scale, color, and shape. The *scale parameter* is an abstract and unitless number that controls the level of homogeneity in image objects created from segmentation. It represents a "degree of fitting", a threshold by which smaller segments are grouped into larger segments while still fulfilling the homogeneity criterion. In other words, smaller segments are grouped into larger

segments as long as the resulting segment maintains a particular threshold of homogeneity; once this threshold is met, the segment is no longer merged with other segments. Segmentations that use a low scale will have many smaller objects that are very homogeneous, while segmentations with higher scales will have larger image objects whose pixels are more heterogeneous. The homogeneity criteria values are chosen through trial-and-error until the chosen parameters result in a satisfactory segmentation.

The *color parameter* defines the amount of spectral information to be used in segmentation, and is the most important parameter for creating meaningful image objects. The color parameter determines the spectral bands to be used for segmentation and how much influence they will have on segmentation. The *shape parameter* is divided into two subcategories, compactness and smoothness. Color is weighted with shape when creating image objects, meaning that more weight or importance placed on one parameter lessens the importance of the other parameter. Compactness and smoothness act together in the same way as do shape and color—when more weight is given to one, less weight must be given to the other. *Smoothness* measures the ratio of the border length of an image object to the border length of an adjacent image object. The smoothness parameter is useful when trying to extract very heterogeneous objects because it helps keep image object borders intact. The compactness parameter uses the ratio of border length to the square root of the number of pixels. This parameter is useful when separating compact objects from other image objects when there is a weak spectral contrast.

The standard deviation of the pixel values in a segment is variable depending on the homogeneity scale chosen (Kim et al., 2008). Finding optimal compactness and smoothness parameters depends on the size and type of object being extracted (Platt and Rapoza, 2008). At least 10% of the criteria used for image segmentation must be given to both the color and shape parameter. However, because an image's spectral characteristics contain the best information for creating image objects, color should be given as much weight as possible while still using shape to achieve useful image objects.

## Classification

Once an image is divided into segments, a classification can be performed. The assumption that an object can only fall into a single category is not always accurate. This is only true if one is performing a deterministic classification (also known as crisp, hard, or binary classifications). Deterministic classifications work only when land cover classes are discrete in nature. By definition a landscape has a continuous and varying surface, and a fuzzy classification could prove a better and more accurate fit than a deterministic classification. With a deterministic classification, misclassification can occur when dealing with pixels that prove difficult to sort into single land cover categories due to their within-class variance. Gaps in the tree canopy, shadows, and other components all comprise part of a land cover class but when included in a segment can confound a deterministic classification (Foody, 1999). Fuzzy classifications allow thematic objects to have varying degrees of membership to one or more land cover categories. Foody (1999)

notes that the degree to which fuzziness is accommodated will be a function of the nature of data sets as well as practical constraints faced by the analyst.

A rule-based hierarchy is used to classify each segment. The rules at the top of a hierarchy trickle down and apply to all sub-classes below it. However, the placement of a segment into a fuzzy classification category is not binary—that is, it is not strictly a "yes" or "no" classification. Rather, a fuzzy-based classification gives each segment a percent chance of inclusion into each class. This technique of classification is appropriate over a landscape, where land cover types are continuous. Using forest classification as an example, fuzzy classification also takes into account error by the producer (e.g. selection of training samples), discrete thresholds set in the classification scheme (e.g. the percent tree cover that equates to forest), and the problem of intraclass variability within the segments (e.g. tree crown vs. tree shadow) (Foody, 1999).

Besides the spectral information present within a satellite image, other information within the image, such as an object's shape, context, or texture can be used to aid in classification. Information about an object's shape can include its size, length-to-width ratio, or perimeter. For example, an object representing a body of water could be classified as a lake or pond. If that object was more defined as a square or rectangle, it might instead be a reservoir; however, based on its small size, it might only be a swimming pool.

Also, the location of an object in an image within the context of other objects around it can help to classify it properly. For example, an object representing an area of grass may be classified as open pasture if it were surrounded by other

objects classified as vegetation. However, if it were surrounded by objects classified as urban features, then it is more likely that it is an urban or suburban park.

Texture refers to the spatial distribution of gray tones or the gray level variation of an image (Haralick et al., 1973; Ferro, 1998). One method of texture analysis is named the Gray Level Co-occurrence Matrix (GLCM), developed by R.M. Haralick (1973; 1979) to analyze the texture of image segments. First-order texture measures are non-spatial and use first-order statistics. Higher order texture calculations are spatial because they use pixel neighbors in calculations; therefore, the placement of pixels within a moving window in relation to each other is significant (Zhu and Yang, 1998). As such, more patterns present on a landscape may be discerned with higher order texture analysis than first order. In this respect, texture can be defined as a placement pattern within an image that is repeated and discernible, and it can be quantified in many ways, including mean, contrast, entropy, and directionality. Measurements of texture are functions of distance and angle. In the simplest terms, GLCM compares the gray level of a pixel (known as the reference pixel) to a pixel neighbor within a moving window, and each pixel within the window is analyzed with regard to its neighbor to detect a textural pattern. Gray values are compared in one or more directions, e.g. east ($0^{o}$), northeast ($45^{o}$), north ($90^{o}$), or northwest ($135^{o}$). The distance of the pixel neighbors to the reference pixel can also vary; pixels may be directly next to each other or a defined distance away from each other.

## Assessing Accuracy and Error

Once an image is classified into a thematic map, its accuracy should be determined before the map is used. There have been many studies that investigate accuracy assessment and recommend the best approach to estimating error, but the reality is that methods for assessing accuracy and error vary between studies (Foody, 2002). Several factors can influence the accuracy of image classification. They include the MMU, sampling scheme, positional accuracy, and thematic accuracy (Stehman and Czaplewski, 1998; Congalton and Green, 1999). MMU refers to the areal point, pixel(s), or polygon used to define reference data. The sampling scheme refers to the method used to collect reference data (discussed in the previous section 'Sampling Design and Data Collection'). These reference data are used as training parameters in classification as well as in accuracy assessment, also referred to by Stehman and Czaplewski (1998) as the evaluation protocol and labeling protocol respectively.

Positional accuracy refers to the actual coordinates of a pixel's location on the ground. It can be affected by image registration errors, terrain, or the angle of the sensor as it captured the image (Congalton and Green, 2009). Positional accuracy can also be compromised when collecting GPS reference data points in the field. Factors such as tree cover, terrain, and atmospheric interference can affect the positional accuracy of collected data. Positional accuracy of GPS data can be improved by using the Position Dilution of Precision (PDOP), a 3-D measure of the quality of GPS data (D'Eon and Delparte, 2005), to set a maximum allowable margin of error.

Thematic accuracy refers to the labeling of a classified image into categories. More specifically, it measures errors of commission (incorrect category label) and omission (not including data into the appropriate category). An error matrix, sometimes called a confusion matrix or contingency table, is a widely-adopted technique used to understand the accuracy of thematic maps produced from imagery (Congalton et al., 1983; Foody, 2002). An error matrix is a square array of numbers that computes producer's, user's, and overall accuracies of a thematic map (Figure 1).

Samples that are correctly classified reside in the error matrix on the major diagonal, and overall accuracy can be determined by dividing the total number of samples by the sum of the major diagonal. Producer's and user's accuracies were first introduced by Story and Congalton (1986) to more adequately display errors of omission and commission. The producer's accuracy is the probability that a selected area on the ground is classified correctly on the map; it resides in the matrix columns. The user's accuracy is the probability that a classified sample on the map is the same as what is on the ground; it resides in the matrix rows. For example, in Figure 1, 71 reference samples were collected that represent the 'Forest' class; of those 71 samples, 45 were correctly classified. This means that of all the forested areas on the image, 63% of that area was classified correctly in the resulting thematic map. On the thematic map, 57 samples were classified as 'Forest'; of those samples, 45 were correct. If a user were to take the thematic map in the field and attempt to locate all forested areas, the user would successfully locate forests 79%

of the time. By including producer's and user's accuracies in addition to the overall accuracy of an error matrix, one is able to pinpoint the classes causing confusion.

| Classified Data | Reference Data: F | A | U | W | Row Totals |
|---|---|---|---|---|---|
| F | 45 | 6 | 1 | 5 | 57 |
| A | 15 | 51 | 11 | 4 | 81 |
| U | 2 | 10 | 82 | 8 | 102 |
| W | 9 | 3 | 15 | 96 | 123 |
| Column Totals | 71 | 70 | 109 | 113 | **363** |

F = Forest
A = Agriculture
U = Urban
W = Water

Overall Accuracy
= 274/363
= 75%

| Producer's Accuracy | User's Accuracy |
|---|---|
| F = 45/71 = 63% | F = 45/57 = 79% |
| A = 51/70 = 73% | A = 51/81 = 63% |
| U = 82/109 = 75% | U = 82/102 = 80% |
| W = 96/113 = 85% | W = 96/123 = 78% |

Figure 1: Example of a deterministic error matrix for a sample-based classification

To quantify the randomness of an error matrix—e.g. is the classification of imagery into a thematic map better than random chance?—a Kappa coefficient can be generated (Cohen, 1960; Congalton et al., 1983). This is a "goodness of fit" test very similar to Pearson's Chi-Square test; it generates a KHAT statistic which measures the chance agreement vs. actual agreement of classes within an error matrix:

$$\hat{K} = \frac{\rho_O - \rho_C}{1 - \rho_C} \tag{4}$$

where: $\hat{K}$ = statistical significance an error matrix
$\rho_O$ = the actual agreement between classes
$\rho_C$ = the chance agreement between classes (Congalton et al., 1983)

KHAT values will range from 0 to 1, with 'zero' being completely chance agreement of classes, and 'one' indicating total statistical agreement of classes. A KHAT value greater than 0.8 represents strong agreement; a value between 0.4-0.8 represents moderate agreement; a value less than 0.4 represents poor agreement (Congalton and Green, 2009).

Traditionally, equally-sized sample units based on pixel size were used as ground reference data, and sample unit counts within classes were used in error matrices. However, there are two influences that should be considered when designing an error matrix: this study makes use of segment-based classifications (as opposed to pixel-based), and uses fuzzy classifications (as opposed to deterministic classifications) and as such, modifications should be made to pixel-based classification error matrices.

Deterministic classifications use a binary model when classifying samples, meaning that a sample either 'is' or 'isn't' classified correctly. However, with fuzzy classifications, samples may have varying degrees of membership to more than one classification category. This concept of "fuzziness" has also been explored relative to accuracy assessment (Congalton and Green, 2009). Instead of a yes/no classification, samples are placed into one of three categories: good, acceptable, and

poor (Figure 2). The 'good' classification for a sample still resides in the major diagonal of the error matrix. However, both the 'acceptable' and 'poor' classifications share the off-diagonal cells of the matrix, and are separated by a comma, respectively. When calculating the fuzzy producer's, user's, and overall accuracies, the 'acceptable' number in the off-diagonal cells (before the comma) are also included.

| Classified Data | Reference Data: F | A | U | W |
|---|---|---|---|---|
| F | 45 | 3,3 | 1,0 | 3,2 |
| A | 6,7 | 51 | 3,8 | 0,4 |
| U | 0,2 | 2,7 | 82 | 6,2 |
| W | 2,7 | 1,2 | 4,11 | 96 |

F = Forest
A = Agriculture
U = Urban
W = Water

Producer's Accuracy (Deterministic)
F = 45/69 = 65%
A = 51/69 = 74%
U = 82/109 = 75%
W = 96/113 = 85%

User's Accuracy (Deterministic)
F = 45/57 = 79%
A = 51/81 = 63%
U = 82/101 = 81%
W = 96/123 = 78%

Overall Accuracy (Deterministic)
= 274/360
= 76%

Producer's Accuracy (Fuzzy)
F = 53/69 = 77%
A = 57/69 = 83%
U = 90/109 = 83%
W = 105/113 = 93%

User's Accuracy (Fuzzy)
F = 52/57 = 91%
A = 60/81 = 74%
U = 90/102 = 89%
W = 103/123 = 84%

Overall Accuracy (Fuzzy)
= 305/360
= 85%

Figure 2: Example of an error matrix used for fuzzy accuracy assessment of a pixel-based classification; producer's, user's, and overall accuracies are compared to a deterministic error matrix

A Kappa analysis works well when all errors in an error matrix are of equal importance, as is the case with a deterministic classification (Congalton and Green, 2009). In the case of a fuzzy classification, a weighted Kappa can be used when errors vary in severity. For example, errors between vegetation strata are less

severe than if a vegetation sample is classified as water or an impervious surface. A weighted KHAT is defined as:

$$\hat{K}_W = \frac{\rho_O^* - \rho_C^*}{1 - \rho_C^*} \tag{5}$$

where: $\hat{K}_W$ = statistical significance of an error matrix
$\rho_O^*$ = the weighted actual agreement between classes
$\rho_C^*$ = the weighted chance agreement between classes (Congalton and Green, 1999)

One way to know if a classification's accuracy is better than random is to calculate a Z-score. This test is defined as:

$$Z = \frac{\hat{K}}{\hat{\sigma}^2} \tag{6}$$

where: $\hat{\sigma}$ = estimate of variance

At a 95% confidence value, if the absolute value of the Z-test is greater than 1.96, the result is better than random.

While both fuzzy classification and fuzzy accuracy assessment have been explored here, they are typically not combined due to the amount of uncertainty introduced into the final thematic map.

# CHAPTER II

# METHODS

This study uses IKONOS satellite imagery to classify land cover via an object-based classification technique. IKONOS is a commercial satellite that has a revisit time of three to five days off-nadir, and approximately 144 days nadir. It is a sun-synchronous satellite that is pointable and able to be tasked, meaning that image acquisition over specific geographic areas can be prioritized. It has a spatial resolution as low as 80cm, and 4 multispectral bands (Table 3).

eCognition©, a proprietary object-based image processing software package developed by Definiens™ and now owned by Trimble™, was used to implement segmentation (FNEA algorithm) and classification of the IKONOS image and produce thematic maps of land cover information in the form of objects. Two thematic maps were produced with eCognition. The goal of each map was to differentiate tree species using IKONOS imagery. The first map depicts forests segmented into individual tree crowns. The second map depicts the forest divided into cover types as described by the SAF (Table 2).

Table 3: Spectral, spatial, and radiometric resolutions of IKONOS-2 sensor

| Band | Spectral (in nm) | Spatial (in $m^2$) | Radiometric |
|---|---|---|---|
| Panchromatic | 526-929 | 0.82 | 11bit |
| Band 1 (Blue) | 445-516 | 3.28 | 11bit |
| Band 2 (Green) | 506-595 | 3.28 | 11bit |
| Band 3 (Red) | 632-698 | 3.28 | 11bit |
| Band 4 (NIR) | 757-853 | 3.28 | 11bit |

* resolution at nadir

## Study Area

From 1750-1850, the New Hampshire landscape was characterized as mostly agriculture, with intense agriculture occurring after 1790 (Foster, 1992). Farm abandonment at the beginning of the industrial revolution allowed for the reforestation of the state. As of 1997, 84% of the state was forested (USFS, 2002). Remnants of this agricultural past remain, most obviously in the form of low stone walls that once divided pastures and farm boundaries (Foster, 1992; Allport and Howell, 1994; Foster and Aber, 2006). New Hampshire has an average growing season of approximately 151 days, receives an average of 120cm of rain each year, and an average of 150cm of snow each year (National Weather Service, 2011).

The study area (Figure 3) is comprised of two distinct parcels of land--Pawtuckaway State Park, a 4,000 acre state-managed park, and 4,600 acres of privately-owned land directly north of the park. The study area is located in the towns of Deerfield and Nottingham, both within Rockingham County, New Hampshire. The IKONOS scene is centered over the greater Mt. Pawtuckaway area. The altitude of the park ranges from 0m (sea level) to 303m (at Mt. Pawtuckaway). The park contains several recreation areas, including hiking trails, swimming, and camping, and is harvested infrequently for timber (Heath, 2008). The private land is

a sparsely settled residential zone, and covered mostly by forest, although several wetland areas exist. Approximately 25% of this private tract of land is actively harvested for timber (Lennartz, 2004).

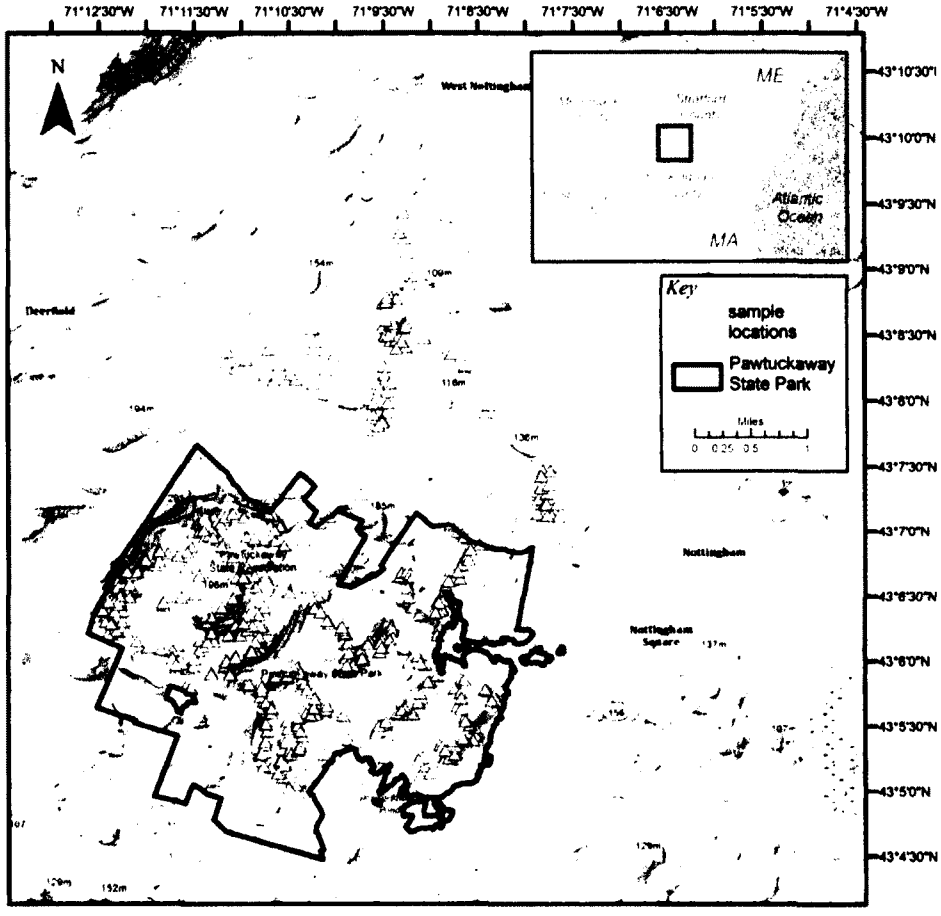


Figure 3: Topographic overview of Pawtuckaway State Park and surrounding study area (Background map sources: USGS, FAO, NPS, EPA, ESRI, DeLorme, TANA)

## Ground Data Collection

Sampling units were collected as 30m x 30m areas. Previous research (Pugh, 1997; Plourde, 2000; Lennartz, 2004; Heath, 2008) had established a composition-based classification scheme for this study area based on the Society of American Foresters (SAF) description of the area (Eyre, 1980); a modified version of this

classification scheme was used for this study (Appendix A). Samples were collected in forested areas. For this study, a forest is defined as having mature and/or immature trees whose crowns touch or are within five meters of each other; forests are at least 1.25 acres in size, and are continuous across the landscape. Forest stands were classified based on the trees represented in the overstory. Trees that did not reach the upper canopy stratum, as judged using visual examination of relative crown positions, were not considered in the classification.

Ground reference sample units were collected during the summers of 2005 and 2006 using a quasi-random sampling technique designed to include as many different forest cover types as possible while staying restricted to roads, trails, and other areas that provided accessibility. Each sample unit represented the center of a $30m^2$ sampling area. Once a plot center point was established, all trees that were within a 15m-radius and reached the top of the canopy were sampled. Ground reference points were collected using a Trimble TDC1 GPS unit. These points were manually corrected for positional accuracy using correction data supplied by a NH Department of Transportation base station in Concord, NH. An additional set of data points, collected in autumn 2007 and following the same collection rules, was also used to supplement existing ground reference points (Heath, 2008).

## Data Preprocessing

A single IKONOS-2 scene with a swath width of 11.3km was used for this study. The scene was acquired by Space Imaging (now GeoEye) on September 5, 2001. The data were geometrically corrected prior to delivery and registered to the

New Hampshire State Plane (FIPS zone 2800, NAD 83 coordinate system). There is some cloud cover present on the image, but is less than 15% of the total image (Figure 4).

Although the image was orthorectified prior to delivery, it was not atmospherically corrected. Aerosol particles in the air can cause light to refract and scatter, confounding image spectra interpretation. Common causes of atmospheric interference include clouds, haze, dust, and smog. Cloud cover is usually too dense to be corrected, and was therefore masked out of the image. To achieve the best possible image for classification, a Top-of-Atmosphere (TOA) correction algorithm was applied to the cloud-free image. This algorithm converts the raw DN (pixel digital number) into reflectance values, allowing index bands to be generated from the original bands for inclusion into segmentation and classification (Dial et al., 2001; Thenkabail, 2004; Chander et al., 2009). This is especially important with the inclusion of derivative bands into an image classification, such as Normalized Difference Vegetation Index (NDVI) (Jensen, 2005; Hagen, 2010).

In a TOA correction, a conversion from raw pixel values to absolute radiance is performed first using the following equation (Chander et al., 2009):

$$L_\lambda = \frac{\mathrm{DN_j}}{CalCoef_j} \tag{7}$$

where: $L_\lambda$ = Spectral radiance at the sensor's aperture [(mW/cm$^2$ sr)]
$\mathrm{DN_j}$ = digital number of $j^{th}$ band [DN]
$CalCoef_j$ = standard calibration coefficient for $j^{th}$ band [(mW/cm$^2$ sr)]

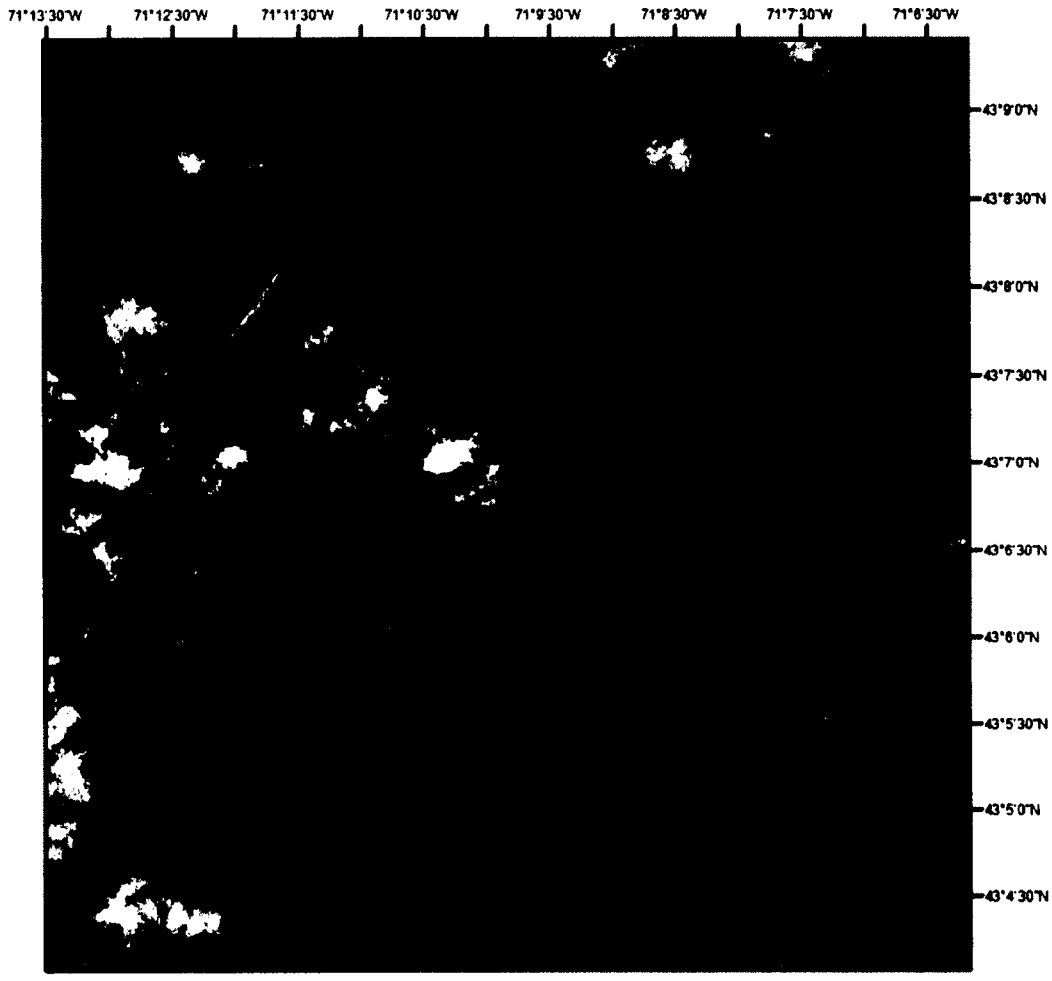


Figure 4: IKONOS false color image showing Pawtuckaway State Park boundaries (south) and privately-owned land parcel (north)

Next, absolute radiance of each pixel is converted to TOA reflectance using the following equation (Chander et al., 2009):

$$\rho_p = \frac{\Pi * L_\lambda * d^2}{\mathrm{ESUN}_\lambda * \cos\Theta_s} \tag{8}$$

where: $\rho_p$ = Planetary reflectance [unitless]
$\Pi$ = 3.14159 [unitless]
$L_\lambda$ = Spectral radiance at the sensor's aperture [mW/ (cm$^2$ sr)]
$d$ = Distance from the sun to the earth [astronomical units]
$\mathrm{ESUN}_\lambda$ = Mean exoatmospheric solar irradiance [mW/ cm$^2$]
$\Theta_s$ = Solar zenith angle [degrees]

In an effort to spectrally separate vegetation features, three vegetation bands were generated in addition to the five original bands: a simple ratio (SR) band that compared the red and NIR spectra, a Normalized Difference Vegetation Index (NDVI), and an Enhanced Vegetation Index (EVI). Also, a principal components analysis (PCA) was performed on the four original multispectral bands in an effort to minimize the correlation of information between the bands (Carleer and Wolff, 2004). By performing a PCA, highly correlated information between bands are transformed into one or more component.

## Segmentation

Segmentation is the crucial "first step" to classifying an image using OBIA because it lays the foundation for classified objects. Nine spectral layers were used in segmentation: the four multispectral bands of the IKONOS image, the panchromatic band, a single principal component created from the original four multispectral bands, and the three vegetation indices. These bands together will be referred to as the pixel level of the image.

When defining the parameters for image segmentation using FNEA (see "Segmentation", pg. 19), the homogeneity criteria of scale, color, and shape are considered. The homogeneity criteria values are chosen through trial-and-error until visual inspection deems a satisfactory segmentation. The initial segmentation groups pixels together until the homogeneity criteria are met. This first segmentation is the most important and will affect the outcome of all subsequent segmentations. Any further segmentation of the image will not begin with the pixel

layer but rather with this initial segmentation by further splitting the segments into sub-objects or grouping segments together into super-objects. Baatz et al. (2004) suggest that because of this, the initial segmentation should create objects as large as possible but as small as necessary. In order to keep track of the different levels of segmentation, each segmentation will be referred to with the 'seg' prefix.

From the pixel level of the image (referred to as seg-A), segmentation progressed over 4 stages. First, large generalized segments were created to separate all vegetation in the image from non-vegetation (seg-B). Second, these large vegetation segments were broken down into sub-objects that delineated individual tree crowns (seg-C). A final segmentation layer was created that grouped tree crowns into forest stands as defined by the SAF land cover classes (seg-D).

| level: | A → | B → | C → | D |
|---|---|---|---|---|
| | pixels → | vegetation → | crowns → | SAF |

Objects in seg-B that were considered 'Non-Vegetation' were not further segmented in seg-C or seg-D.

## Training and Classification

A class hierarchy was created to classify the image based on the modified SAF schema (Table 4). To differentiate between the different class hierarchies, the prefix 'tier' will be used. For all segmentations, two parent classes were initially created, 'Vegetation' and 'Non-Vegetation', to isolate all non-forest aspects of the image and remove their influences on species-specific forest classifications (tier-1 schema). Non-vegetated areas include open water, roads, buildings, and bare ground. The

'Vegetation' class was further divided into 'Forested' and 'Non-Forested' (tier-2 schema). Examples of non-forested categories present in the IKONOS image include grassy fields, some wetlands, and early successional growth. The seg-B segmentation was classified using tiers 1&2 class hierarchy. Training areas for seg-B objects were chosen by visually interpreting the IKONOS image. Seg-C objects were classified to tree species, and seg-D objects were grouped into super-objects and classified according to the SAF-defined classes (tier-4 schema). Both seg-C and seg-D training data were collected via field sampling.

Table 4: eCognition© class hierarchy used for classification

| *Tier 1* | *Tier 2* | *Tier 3* | *Tier 4* | *Description* |
|---|---|---|---|---|
| Vegetation | Forested | Evergreen | WP | White Pine |
| | | | HE | Hemlock |
| | | | WH | White Pine/ Hemlock |
| | | Deciduous | BH | Beech |
| | | | RM | Red Maple |
| | | | OAK | Oak |
| | | | OTHER | Other Deciduous Forest |
| | | Mixed | MX | Mixed Forest |
| | Non-Forested | *(n/a)* | NF | Non-Forest |
| Non-Vegetation (including clouds) | (Excluded from further classification) | | | |

Ground reference data were transferred from the GPS unit to an ArcGIS shapefile. Each point contained attributes of tree species found at the location (if it was a forested site) and other descriptive data. A total of 250 points out of 522 collected in the field were chosen to serve as training areas. These training samples were imported into eCognition© as a TTA (training and test area) mask. Once the

TTA mask was created, it was linked to the class hierarchy and could then be converted into training samples within eCognition©.

A divergence analysis was performed, called Feature Space Optimization (FSO) within eCognition©, to find the features that would best classify the segments (Appendix B). Divergence analysis is a statistical method used to select features that best separate two or more classes (Jensen, 2005). By optimizing the feature space, features were selected that best separate polygons into classes (Leduc, 2004; Durrieu et al., 2007). These features were then added to the classes as a nearest neighbor (NN) classifier. Nearest neighbor classifiers evaluated feature space overlap between samples and also managed overlaps during classification (Baatz et al., 2004). These overlaps in feature space were what allowed polygons to have fuzzy memberships to more than one class. eCognition© uses two types of nearest neighbor classifiers: standard NN and class-specific NN. By using the standard NN approach, features that were deemed optimal for class separation were applied to all classification categories equally; class-specific NN allows different optimal features to be applied to different classification categories (Baatz et al., 2004; Leduc, 2004). For this study, the standard NN was modified.

Training areas were chosen so that samples were evenly distributed over the map. Polygon samples for seg-B objects included homogeneous areas such as grassy fields and closed canopy forest, as well as mixed samples such as polygons that grouped forest and open fields. The largest source of mixed samples was land cover edges and shadows created by tree canopy gaps. Segments that were classified as 'Non-Vegetation' in seg-B were not included in further classifications (Figure 5).

Each of the classified segmentations was exported as an ArcGIS shapefile to be used for accuracy assessment.

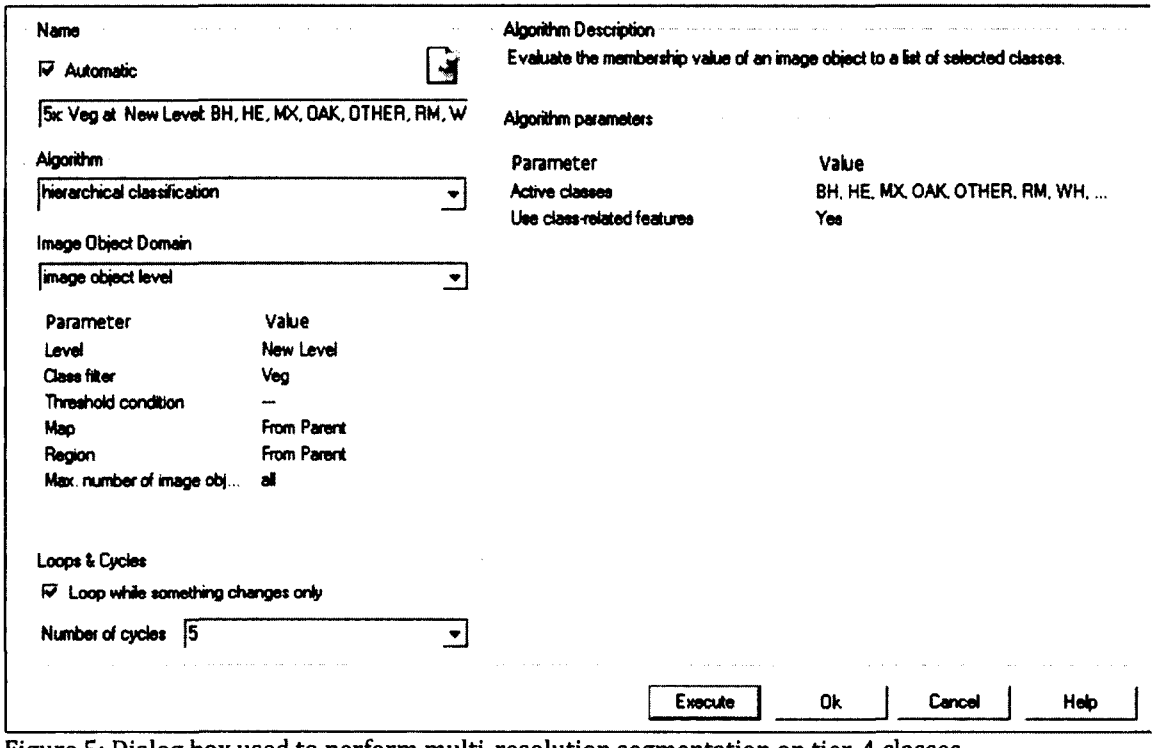

Figure 5: Dialog box used to perform multi-resolution segmentation on tier-4 classes

## Accuracy Assessment

A thematic accuracy assessment was performed using a fuzzy error matrix. Because no such method for accuracy assessment exists within eCognition©, the classified objects were exported to a polygon shapefile; objects not used for classification training were used to perform an accuracy assessment.

When collecting and organizing reference data, consideration was given to what would be the 'best' classification, but also to what would be an 'acceptable' classification. Also, because eCognition© uses a fuzzy logic when classifying imagery, it assigns each segment a degree of certainty pertaining to each possible

class. To account for 'best' and 'acceptable' classes in both the reference data and the map data, three error matrices were generated for the 'SAF' classification. The first imposed the strictest rules regarding classification accuracy. It only analyzed what the reference data considers the 'best' class, and compares it to what eCognition© ranked the most likely class. The second error matrix was less strict—it analyzed what the reference data considered 'best' and 'acceptable' classes, and compared it to what eCognition© considered the most likely class. The third error matrix was the least strict, or the most "fuzzy", in regards to accuracy. It not only analyzed what the reference data considered 'best' and 'acceptable' classes, but it also considered eCognition's second ranked class as well as the highest ranked. Producer's accuracy, user's accuracy, and overall accuracy were also determined for each error matrix. To test the statistical significance of each accuracy assessment, a Kappa statistic was also calculated.

# CHAPTER III

# RESULTS

## Segmentation

Steps taken for each segmentation are summarized below (Table 5). In the seg-B stage of segmentation (called level 1), pixels were grouped into polygons that were either 'Vegetation' or 'Non-Vegetation' (Figure 6). Ninety percent of the homogeneity criteria were given to color and only 10% to shape since reflectance values were more important than shape. The shape criterion remained equally split, with 50% going to smoothness and 50% given to compactness. The NIR band and the NDVI band were the only bands used to create the objects within seg-B.

Table 5: Parameters used for segmentation

| *Segmentation* | *Level* | *Bands Used* | *Scale* | *Color* | *Shape* | | *Accept-able?* |
|---|---|---|---|---|---|---|---|
| | | | | | *Comp.* | *Smooth* | |
| Seg-B | 1 | NIR<br>NDVI | 30 | 0.9 | 0.5 | 0.5 | Yes |
| Seg-C | 2a | Panchromatic<br>Principal Component | 18 | 0.6 | 0.5 | 0.5 | No |
| | 2b | Green<br>Red<br>NIR | 18 | 0.8 | 0.5 | 0.5 | No |
| | 1b | Panchromatic<br>Principal Component | 18 | 0.6 | 0.5 | 0.5 | No |
| Seg-D | 2c | All bands except Panchromatic | 25 | 0.8 | 0.5 | 0.5 | Yes |

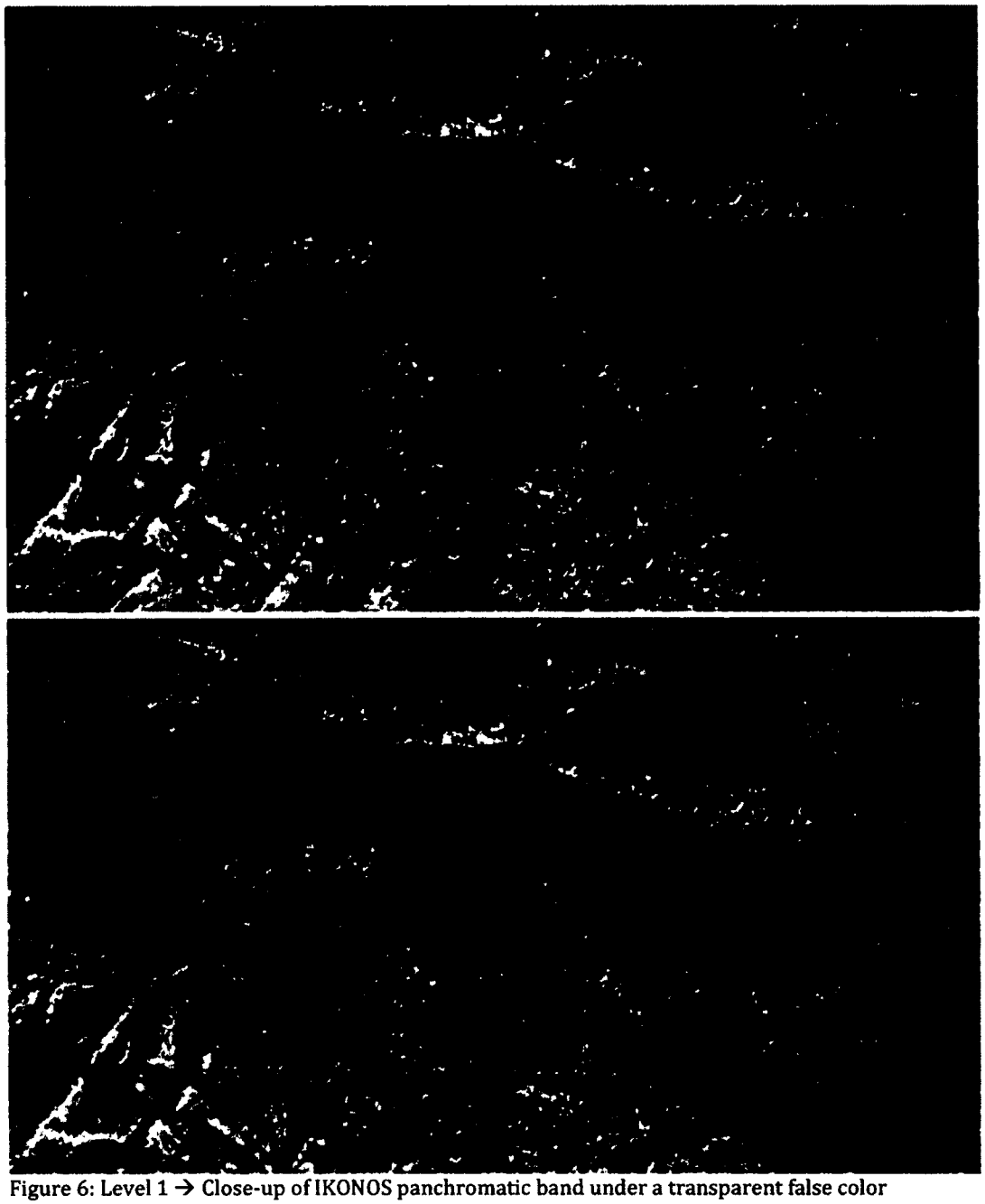

Figure 6: Level 1 → Close-up of IKONOS panchromatic band under a transparent false color composite (above) and with seg-B "vegetation-nonvegetation" results (yellow outline, below)

Using objects created from seg-B, sub-objects were created using the panchromatic and principal component band (called level 2a). Because seg-C was concerned with tree crown extraction, the panchromatic band was used because of its higher spatial resolution, and principal component band was used because it contained decorrelated information regarding spectral characteristics (Figure 7). A second attempt was made using the green, red, and near infrared bands (level 2b) (Figure 8). However, in repeated attempts at creating seg-C, both the panchromatic band and the principal component band created objects that most closely resembled tree crowns in comparison to all other segmentation attempts that used different bands. Creating tree crown objects directly from the pixel level—that is, going from seg-a directly to seg-C—did not prove useful (level 1b) (Figure 9). Approximately fifty different combinations of homogeneity and shape/color values were tested for tree crown segmentations. The best segmentation used both the principal component (PC) band and the panchromatic band with each given equal layer weights. All other bands were given a layer weight of zero (and therefore not considered in the initial segmentation). Giving either the panchromatic band or the PC band more weight than the other resulted in less-than-optimal results. Different color and shape parameters were also experimented with. Giving less than 40% weight to the color criterion produced meaningless segments. Ultimately, it was found that giving color 60% weight yielded the best results. More than 830,000 objects were created in seg-C segmentation .

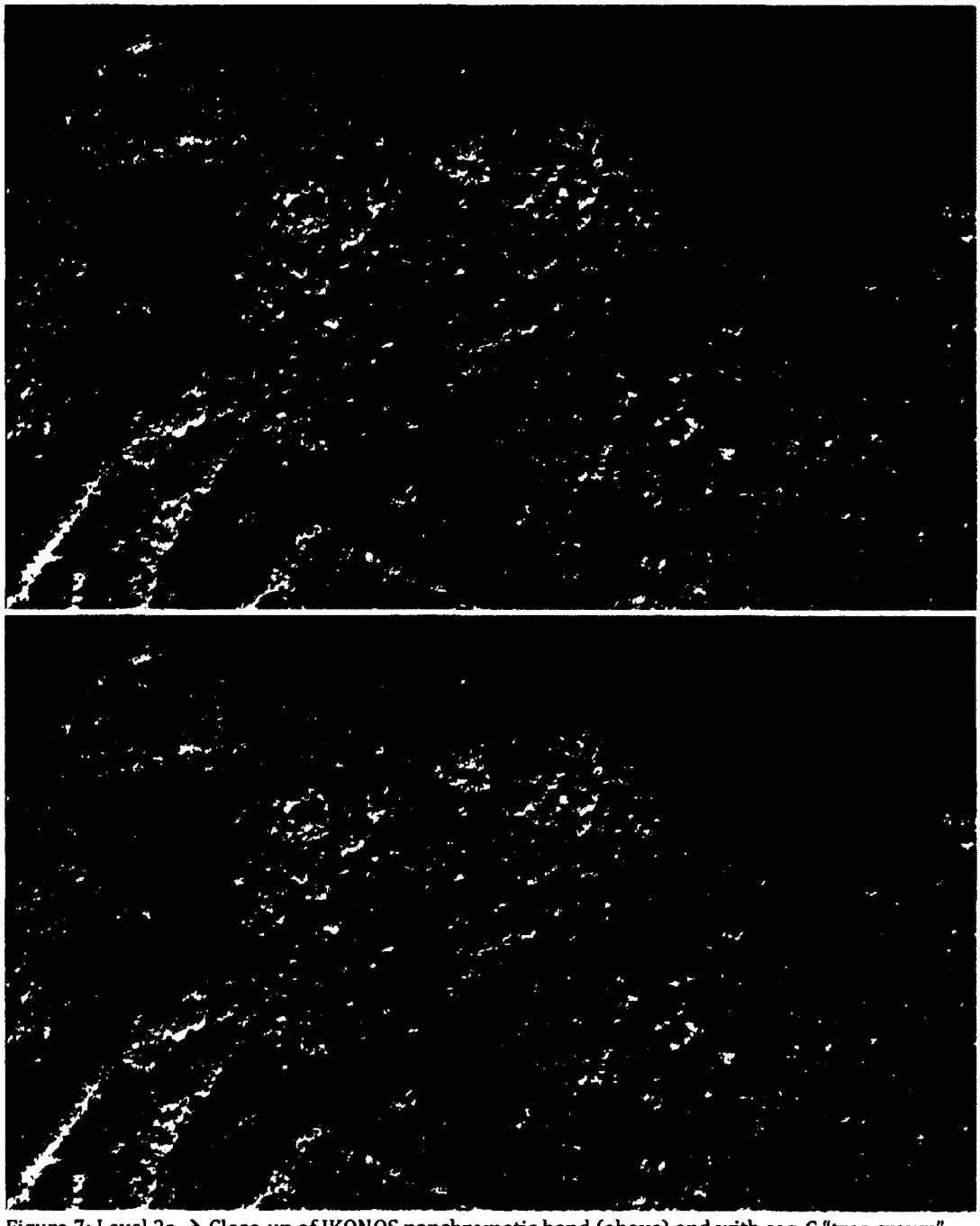

Figure 7: Level 2a → Close-up of IKONOS panchromatic band (above) and with seg-C "tree crown" results (yellow outline, below)

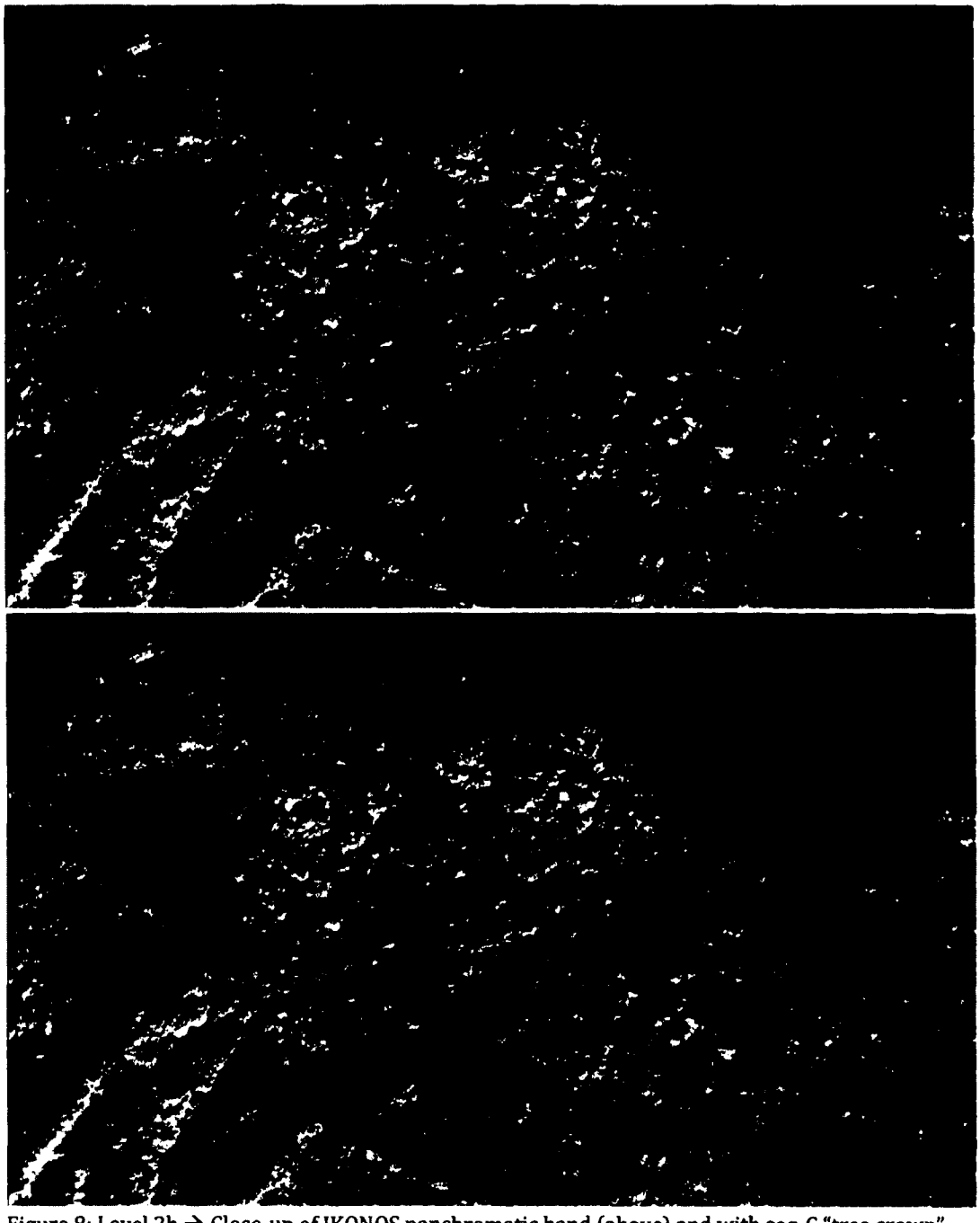

Figure 8: Level 2b → Close-up of IKONOS panchromatic band (above) and with seg-C "tree crown" results (yellow outline, below)

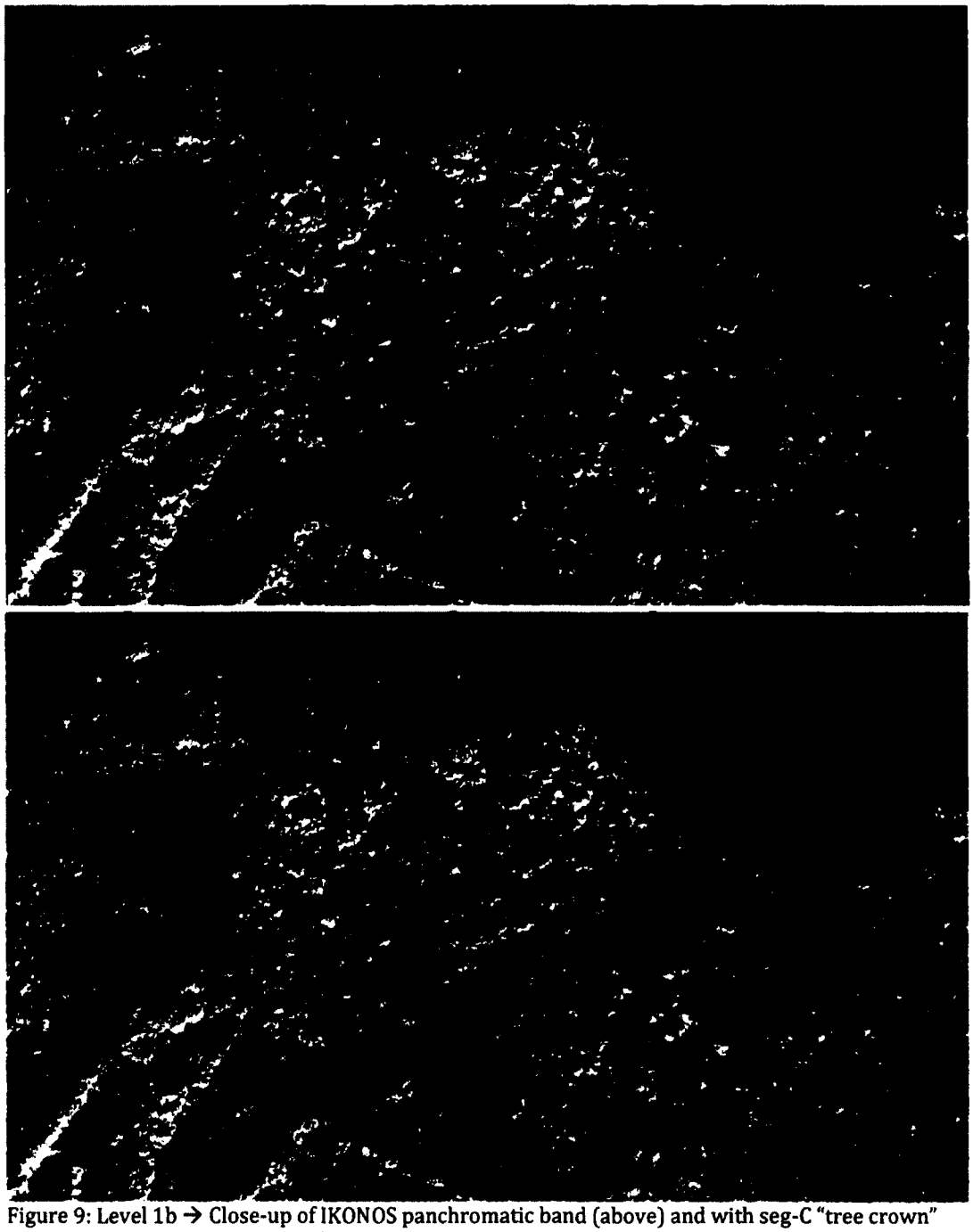

Figure 9: Level 1b → Close-up of IKONOS panchromatic band (above) and with seg-C "tree crown" results (yellow outline, below)

The spatial resolution of the IKONOS image was enough to discern only the largest tree crown diameters in the image (Figure 10). As a result, the majority of tree crowns were either over- or under-segmented. Seg-C results were overlaid with the IKONOS image and a "leaf-on" aerial image from 2004 with a spatial resolution of 0.5 $ft^2$ (Figure 11). Upon visual inspection in both field-sampled and non-sampled areas, there was no difference found in segmentation results when comparing level 1b to other seg-C segmentations; a bottom-up approach (small objects to big objects) yielded no better results than a top-down approach. Objects were generated that resembled tree crowns, but edges between land cover types weren't defined properly. Despite multiple attempts at segmentation, seg-C segmentations were inadequate at defining actual tree crowns. Therefore, seg-C was abandoned (Table 5).

Because tree crown delineation was unsuccessful, seg-D was created directly from seg-B. In seg-D, objects classified broadly as vegetation were sub-divided into forest stands based on SAF classification guidelines. Unlike all previous segmentations, the best results were achieved for seg-D by including all bands except the panchromatic band in the segmentation (Figure 12). Inclusion of the panchromatic band did not affect the segmentation, but did significantly slow down the processing speed. Again, the shape criterion remained equally split between compactness and smoothness. For seg-D, several iterations of segmentation with different combinations of bands were attempted—e.g. the PC and panchromatic bands alone, vegetation indices alone, different layer weights vs. equal weights, etc. The shape parameter was also varied in trial segmentations, with the compactness

and smoothness criteria were given various weights—extreme values in either direction as well as only moderate shifts. However, weighting the shape criteria with anything other than equal weight yielded oddly-shaped polygons that did not resemble tree stands. This segmentation generated 143,171 objects (Figure 13).

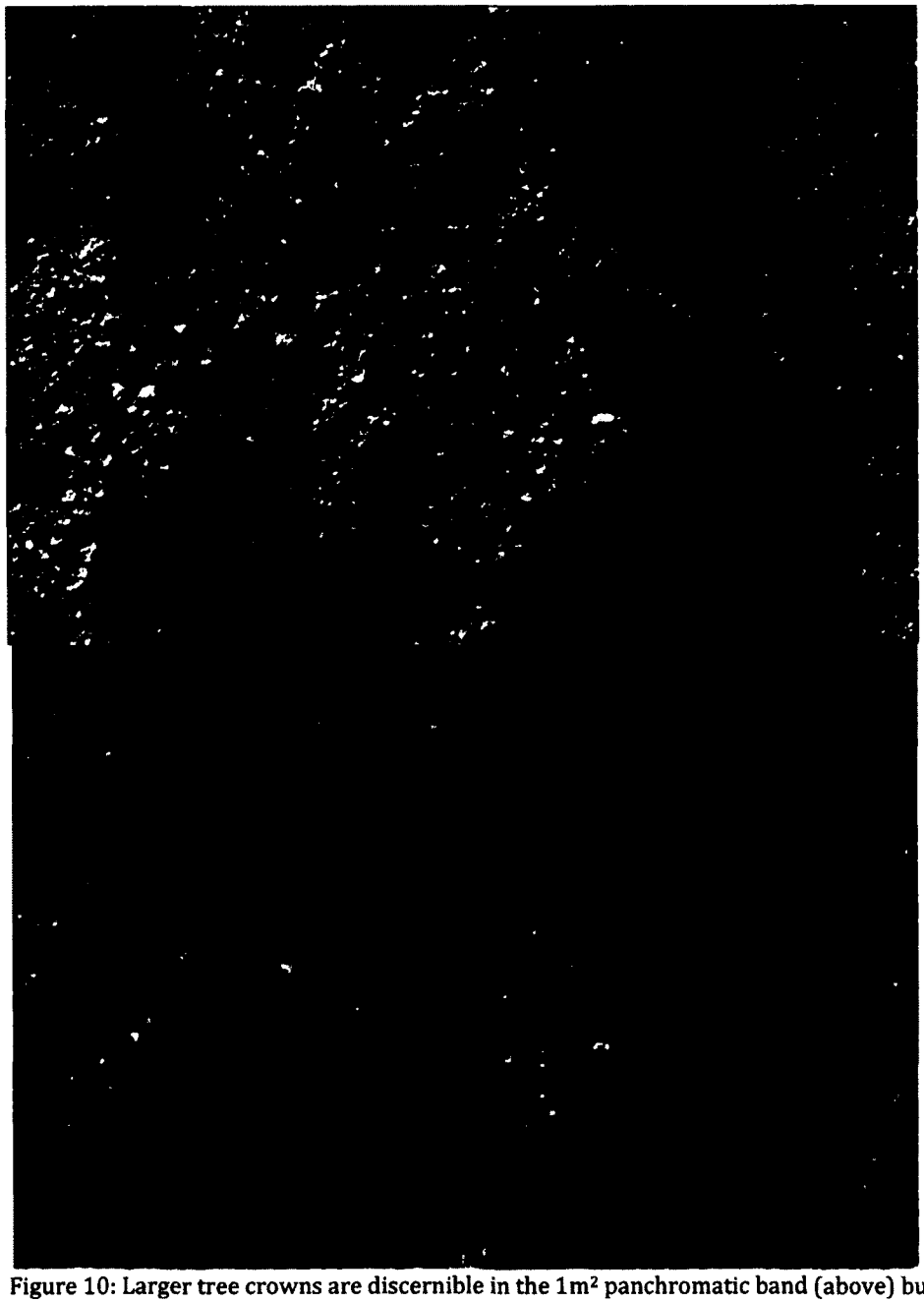

Figure 10: Larger tree crowns are discernible in the $1m^2$ panchromatic band (above) but not in the $4m^2$ multispectral bands (below)

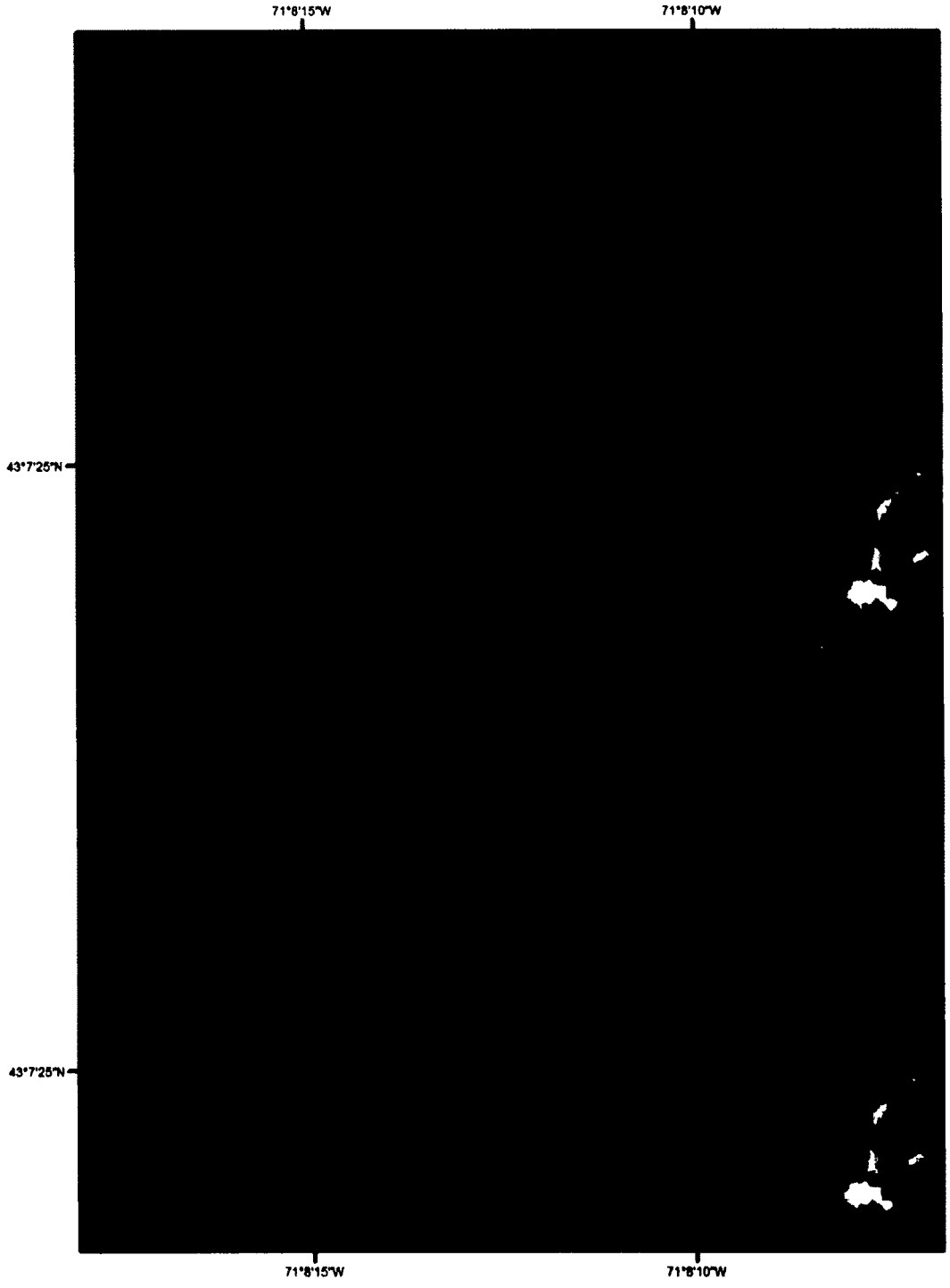


Figure 11: View of Pawtuckaway aerial images with seg-C (level 2a) segments (below) and without segments (above)

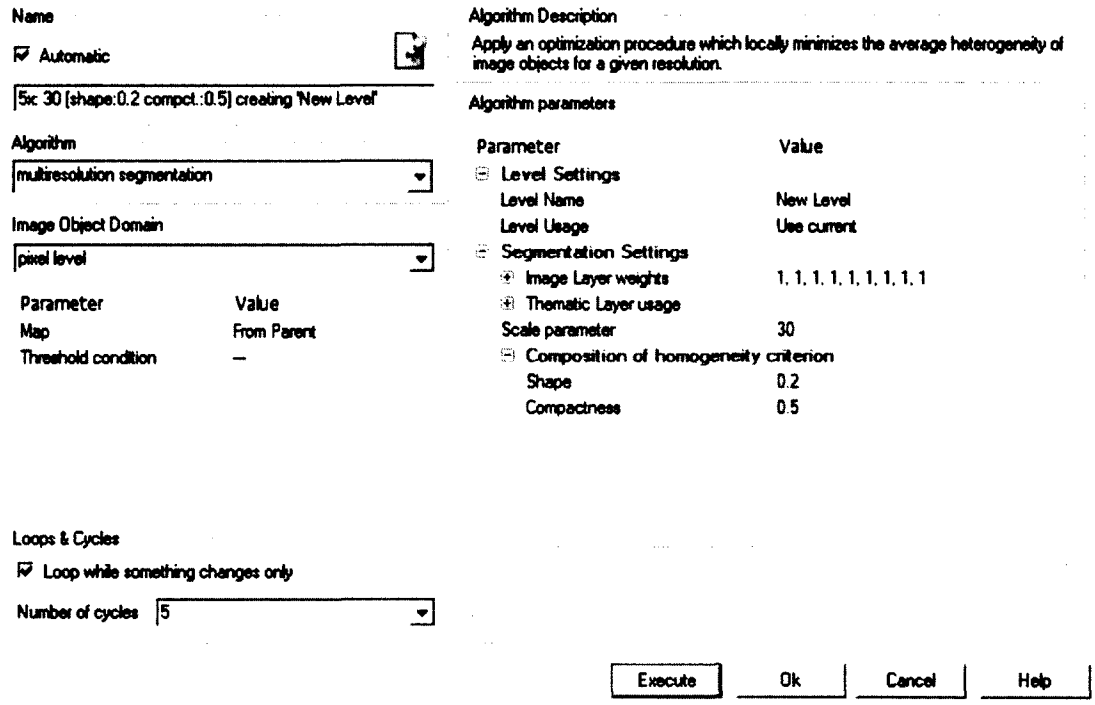

Figure 12: Parameters used to create seg-D segmentation

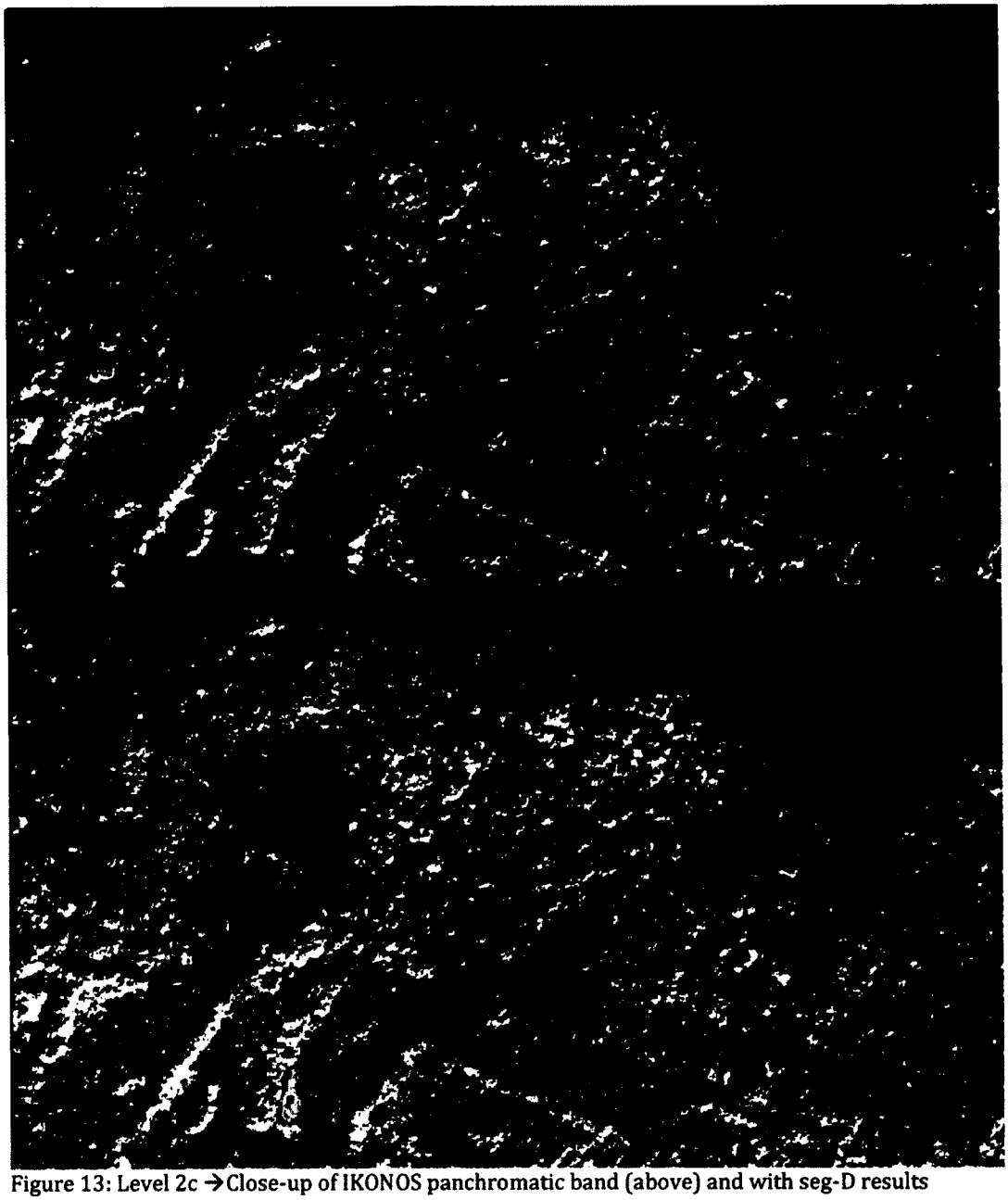

Figure 13: Level 2c →Close-up of IKONOS panchromatic band (above) and with seg-D results (yellow outline, below)

## Training and Classification

eCognition© uses a modified supervised classification technique. A divergence analysis (called 'Feature Space Optimization, or FSO) was used to determine the best separation between classes. For Vegetation and Non-Vegetation classes, thirty-seven features were used in the analysis (Appendix B). A maximum of 10 dimensions were analyzed and separation was achieved using nine dimensions, which were applied to the nearest neighbor descriptor and added to each class description. Larger values mean better separability; nine dimensions resulted in a separability distance of 12.049 (Figure 14).

Due to computational limitations, dimensional constraints were imposed for seg-D (tier-4 class analysis, see pg. 39 for description). Thirty-seven features were analyzed in maximum of ten dimensions (Figure 15). Separation distances were not as large between tier-4 classes as they were between vegetation and non-vegetation; the separability distance was 1.56. Analysis of the seg-D class feature space could not reach a maximum distance needed for separation with only ten dimensions. The feature space can be analyzed in only as many directions as there are features. If allowed to use as many dimensions in the feature space as there are features, twenty-two dimensions would have been selected out of a possible thirty-seven. However, the distance would have only increased to 1.8 from 1.56. There was insignificant improvement in classification when twenty-two dimensions were used versus ten; the minimal increase in the feature space did not improve classification results significantly to warrant the trade-off between feature space distance and time/computational power.

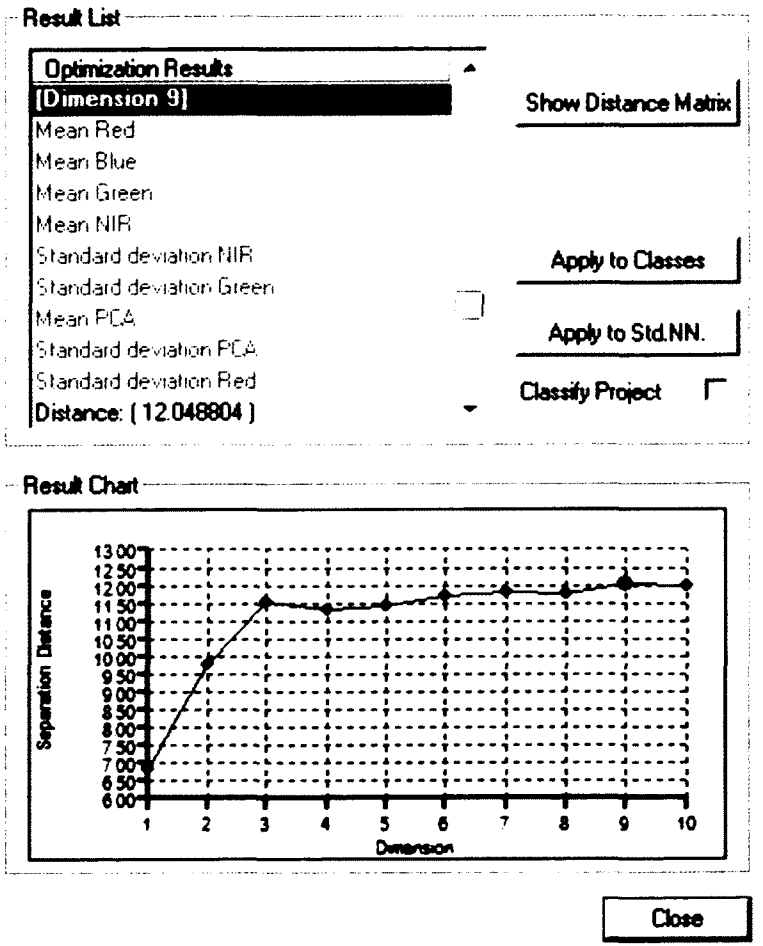


Figure 14: Nine dimensions used to separate vegetation from non-vegetation

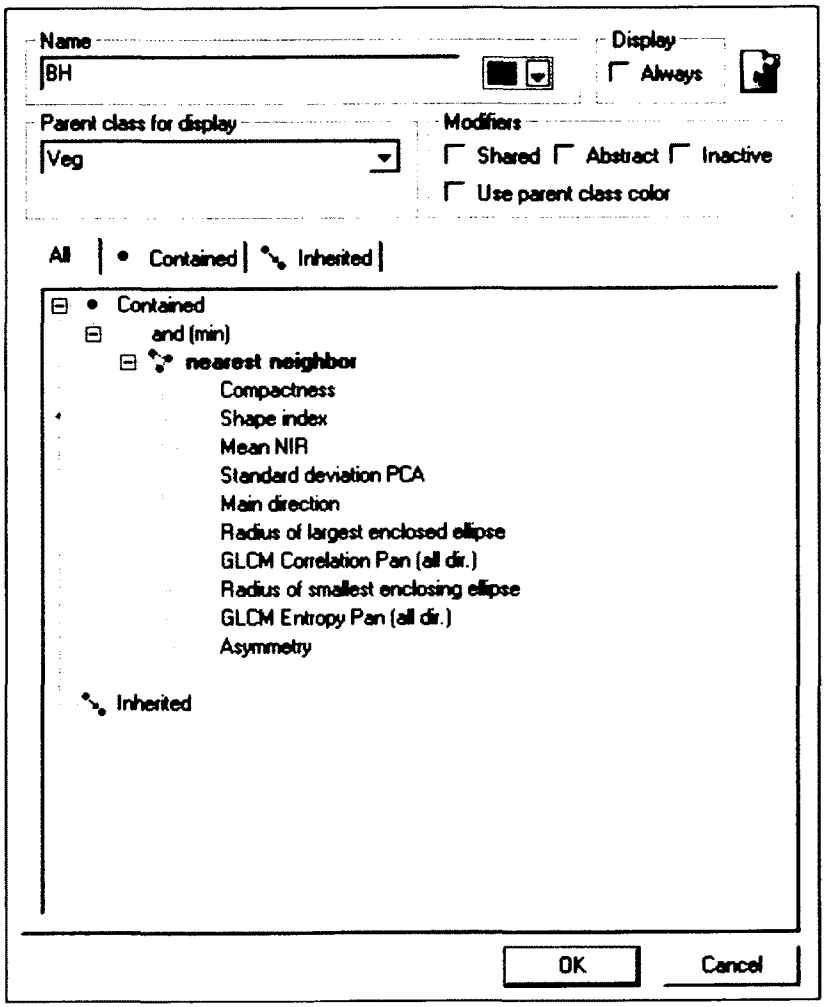


Figure 15: Ten dimensions used to separate tier-4 classes

## Accuracy Assessment

Three error matrices were generated for the 'SAF' classification. The first (Table 6) imposed the strictest rules regarding classification accuracy ('best' classes from classification and reference data). The second error matrix (Table 7) was less strict (used 'best' and 'acceptable' classes from reference data, and 'best' classes from classification). The third error matrix (Table 8) was the least strict ('best' and 'acceptable' classes from both classification and reference data). Unlike Figure 2 (pg. 29) which shows the best and acceptable samples separately in the major diagonal, the best and acceptable samples in the second and third error matrices were added together. The overall accuracy for each matrix was poor, and ranged between 32-46%. The class that was the hardest to discern was mixed forest ('MX'). This is understandable since segments are homogeneous in nature and mixed forest is heterogeneous by definition. Non-forested vegetation had the highest accuracies, perhaps because it is a broadly defined class or is less spectrally variable.

A Kappa analysis (Equation 4, pg. 28) was performed to measure the level of agreement between the thematic map and the reference data. A Z-test (Equation 6, pg. 30) was also performed to determine if the classification was better than random. These analyses were executed for each of the three error matrices generated (Table 9). Matrix 3, which had the most relaxed rules regarding correct sample classification, has a KHAT value over 0.4, indicating a moderate agreement between the reference data and the classification. Matrices 1 & 2, however, had poor agreement between the reference data and each classification. However, all

three classifications were better than random at a 95% confidence level, as indicated by a Z-score higher than 1.96.

Table 6: MATRIX 1—error matrix applying the strictest rules for class membership—analyzed the 'best' class from both the reference data and eCognition©

| Image Classification \ Ground Reference | NF | WP | HE | WH | OAK | BH | RM | MX | OTHER | Row Totals | User's Accuracy |
|---|---|---|---|---|---|---|---|---|---|---|---|
| NF | 15 | 7 | 0 | 1 | 3 | 0 | 0 | 0 | 0 | 26 | 57.69% |
| WP | 1 | 20 | 1 | 0 | 7 | 1 | 2 | 0 | 0 | 32 | 62.50% |
| HE | 2 | 5 | 4 | 0 | 9 | 3 | 3 | 1 | 2 | 29 | 13.79% |
| WH | 1 | 5 | 1 | 6 | 5 | 1 | 2 | 2 | 0 | 23 | 26.09% |
| OAK | 5 | 9 | 4 | 4 | 10 | 5 | 2 | 10 | 5 | 54 | 18.52% |
| BH | 1 | 3 | 2 | 1 | 4 | 10 | 1 | 1 | 3 | 26 | 38.46% |
| RM | 1 | 3 | 3 | 3 | 10 | 2 | 9 | 5 | 4 | 40 | 22.50% |
| MX | 2 | 0 | 0 | 0 | 1 | 0 | 1 | 1 | 1 | 6 | 16.67% |
| OTHER | 0 | 2 | 2 | 0 | 1 | 3 | 0 | 1 | 5 | 14 | 35.71% |
| Column Totals | 28 | 54 | 17 | 15 | 50 | 25 | 20 | 21 | 20 | 250 | |
| Producer's Accuracy | 53.57% | 37.04% | 23.53% | 40.00% | 20.00% | 40.00% | 45.00% | 4.76% | 25.00% | | |

Overall Accuracy: 32.00%

Table 7: MATRIX 2—error matrix analyzing the 'best' and 'acceptable' classes from the reference data, and the 'best' class from eCognition©

| Image Classification \ Ground Reference | NF | WP | HE | WH | OAK | BH | RM | MX | OTHER | Row Totals | User's Accuracy |
|---|---|---|---|---|---|---|---|---|---|---|---|
| NF | 16 | 6 | 0 | 1 | 2 | 0 | 0 | 0 | 0 | 25 | 64.00% |
| WP | 0 | 31 | 1 | 0 | 6 | 1 | 1 | 0 | 0 | 40 | 77.50% |
| HE | 2 | 5 | 5 | 0 | 8 | 3 | 3 | 1 | 2 | 29 | 17.24% |
| WH | 1 | 1 | 0 | 6 | 4 | 1 | 2 | 1 | 0 | 16 | 37.50% |
| OAK | 5 | 4 | 4 | 4 | 17 | 5 | 1 | 7 | 5 | 52 | 32.69% |
| BH | 1 | 3 | 2 | 1 | 3 | 10 | 1 | 1 | 3 | 25 | 40.00% |
| RM | 1 | 2 | 3 | 3 | 9 | 2 | 12 | 5 | 4 | 41 | 29.27% |
| MX | 2 | 0 | 0 | 0 | 0 | 0 | 0 | 5 | 1 | 8 | 62.50% |
| OTHER | 0 | 2 | 2 | 0 | 1 | 3 | 0 | 1 | 5 | 14 | 35.71% |
| Column Totals | 28 | 54 | 17 | 15 | 50 | 25 | 20 | 21 | 20 | 250 | |
| Producer's Accuracy | 57.14% | 57.41% | 29.41% | 40.00% | 34.00% | 40.00% | 60.00% | 23.81% | 25.00% | | |

Overall Accuracy: 42.80%

Table 8: MATRIX 3—error matrix with the most relaxed rules—analyzed the 'best' and 'acceptable' classes from both the reference data and eCognition©

| Image Classification \ Ground Reference | NF | WP | HE | WH | OAK | BH | RM | MX | OTHER | Row Totals | User's Accuracy |
|---|---|---|---|---|---|---|---|---|---|---|---|
| NF | 17 | 6 | 0 | 1 | 2 | 0 | 0 | 0 | 0 | 26 | 65.38% |
| WP | 0 | 31 | 1 | 0 | 6 | 1 | 1 | 0 | 0 | 40 | 77.50% |
| HE | 2 | 5 | 5 | 0 | 8 | 3 | 3 | 1 | 2 | 29 | 17.24% |
| WH | 1 | 1 | 0 | 7 | 4 | 1 | 2 | 1 | 0 | 17 | 41.18% |
| OAK | 5 | 4 | 4 | 3 | 20 | 5 | 1 | 6 | 4 | 52 | 38.46% |
| BH | 1 | 3 | 2 | 1 | 3 | 10 | 1 | 1 | 3 | 25 | 40.00% |
| RM | 1 | 2 | 3 | 3 | 6 | 2 | 13 | 5 | 4 | 39 | 33.33% |
| MX | 1 | 0 | 0 | 0 | 0 | 0 | 0 | 5 | 1 | 7 | 71.43% |
| OTHER | 0 | 2 | 2 | 0 | 1 | 2 | 0 | 1 | 7 | 15 | 46.67% |
| Column Totals | 28 | 54 | 17 | 15 | 50 | 24 | 21 | 20 | 21 | 250 | |
| Producer's Accuracy | 60.71% | 57.41% | 29.41% | 46.67% | 40.00% | 41.67% | 61.90% | 25.00% | 33.33% | | |

Overall Accuracy: 46.00%

Table 9: KHAT and Z-score statistics for three classifications

| | KHAT | Variance | Z-score |
|---|---|---|---|
| Matrix 1 | 0.22232 | 0.00117 | 6.50562 |
| Matrix 2 | 0.34300 | 0.00127 | 9.62987 |
| Matrix 3 | 0.49449 | 0.00126 | 13.94204 |

# CHAPTER IV

# DISCUSSION AND SUMMARY

This work was begun in 2004 when OBIA was in its infancy. Little was known about the classification process and the issues surrounding assessing the accuracy of segment-based maps were poorly understood. Since then, object-based image analysis has been demonstrated to be a powerful tool in classifying high resolution imagery, and understanding of OBIA-based image classification has advanced.

## Collection of Reference Data

In hindsight, there were several factors that limited OBIA's success in this study. The first factor involves the collection of ground reference data. Individual points were collected as a representation of $30m^2$ forest canopy cover. However, these data were collected prior to the publication of any formal arguments on the proper collection of ground data points as it pertains to object-based classification. Objects are different in size and shape, and are not each 30x30m plots. By segmenting the image prior to field data collection, the object would have been the most appropriate sample unit.

Ground reference data were initially collected in 2005-2006 and combined with ground reference data collected in 2007 by Heath (2008). However, since these data were collected prior to segmentation, many points were unable to be used due to spatial autocorrelation or multiple points within one segment. Therefore, the 50 sample minimum suggested by Congalton and Green (2009) was not met. This further supports the idea that segmentation should occur prior to ground reference data collection. In general, it is often impractical or impossible to collect the minimum required sample units due to such constraints as time, money, or access, especially if the image is dominated by mixed pixels, mixed classes, or both (Foody, 1999). Grenier et al. (2008) proposed a modification of the 50-samples-per-class rule to redistribute the sampling effort to reflect the effort needed for accurate classification, ensuring that 50 samples x *n* classes are collected but giving more samples to classes where there are larger in-class variations.

## Classification Scheme

Sample units were collected based on guidelines set by the SAF to describe and classify New England forests. These are the classification guidelines used by the State of New Hampshire as well as previous classification studies of the Pawtuckaway area (Pugh, 1997; Plourde, 2000; Lennartz, 2004). For the purposes of continuity, the same classification scheme was chosen in 2004 for this study.

Ideally, classification schemes by definition should be mutually exclusive and totally exhaustive, and should also contain not only labels, but definitions of each class as well (Congalton and Green 2009). In practice, it is rare that a classification

scheme meets all of these criteria. As a result, mapping the ground using a classification scheme can be difficult and mapping using remote sensing techniques even more difficult. The SAF's definitions of northeastern U.S. forest stand classes were not mutually exclusive (e.g. four of the SAF's definitions include Eastern White Pine as a dominant species, and two of those four also contain Eastern Hemlock as a dominant species); this scheme is appropriate for forest management and on-the-ground assessment, but not ideal for remote sensing applications. In an effort to make these classes more exclusive for this study, the rules were rewritten into a dichotomous key (Appendix A). Despite these modifications, this classification scheme remained problematic for labeling many of the forested areas in this study. First, the basis of these guidelines lies in the composition of the entire forest stand, including trees that may not be part of the forest canopy/overstory (and therefore not visible in satellite images). Even though these guidelines were modified for this particular study, there was still too much reliance on the presence of species that were simply not canopy-dominant within the study area.

## Accuracy Assessment

It was mentioned (pg. 28) that two study-specific influences should be considered when designing an error matrix. One was that the study bases accuracy on fuzzy classifications, and this was considered in the types of error matrices used. But the other influence, that the study uses objects instead of pixel-based sample units, was not considered in the error matrix design. This is a new concept that was

not taken into account in early OBIA studies, and therefore wasn't considered in 2004 when this study was conducted.

In a pixel-based classification, all samples in the error matrix are identical in size. In an object-based classification, however, polygons are samples in the error matrix, and may not be the same size or shape as the ground reference sample. This use of equal area samples to interpret polygons of unequal size results in a biased accuracy assessment, and overall accuracy of the thematic map cannot be computed with a traditional error matrix (Radoux et al., 2011). This is an evolving area of research and analysis and the proper handling of error matrices in this case is not entirely clear. One way to alleviate the effects of differently-sized polygons in accuracy assessment is to segment the image before collecting ground reference samples. This segmentation can be used to choose where and how many samples should be collected for each land cover class as well as how many samples should be collected within each segment.

Area-based error matrices have been discussed in the literature (Whiteside et al., 2010; Radoux et al., 2011), but there are no concrete examples of their use or a measure of their statistical significance. Nevertheless, a predictor of overall area-weighted accuracy is offered:

$$\pi = \frac{1}{S_T}\left(\sum_{i=1}^{n} C_i S_i + \rho \sum_{i=n+1}^{N} S_i\right) \tag{9}$$

where: $\pi$ = overall area-weighted classification accuracy
$\rho$ = weighted probability that object $n$ will be correctly classified
$C_i$ = binary classification of the map object (1=correct, 0=incorrect)
$S_i$ = area of the map object
$S_T$ = the total surface of the map
$N$ = total objects $n$ on the map
(Radoux et al., 2011)

Further study of this application would be advantageous to future OBIA studies.

## Other Remarks

The first objective of this study was to delineate individual tree crowns as a method to build more accurately-depicted forest stands. This was not achieved due to limitations in the spatial resolution of the imagery. The spatial resolution of the IKONOS sensor is not high enough to accurately distinguish between tree crowns, especially small or young trees, or dense forest where the edges of tree crowns intermingle with the edges of tree crowns around it. Incorporating spectral information to separate tree crown edges might solve this problem if the spectral resolution of the sensor is high enough. Bands within the infrared spectrum have been used to identify different vegetation characteristics such as 'greenness' and phenology characteristics, and also allow for separation from background interference such as soil (Tucker, 1979). IKONOS has only one band in the near infrared spectrum and three bands in the visible region of the spectrum. In comparison, NASA JPL designed AVIRIS (Airborne Visible InfraRed Imaging Spectrometer) to collect 224 continuous bands from 350-2500nm, each with a

bandwidth of approximately 10nm. Hyperspectral sensors such as AVIRIS have been used to differentiate different forest cover types (Martin et al., 1998; Plourde et al., 2007). IKONOS does not have the spectral resolution required to distinguish differences in cover types reliably and with sufficient accuracy; more bands in the infrared region might help to distinguish between forest cover types. Accurately delineating single-species objects might provide better ground reference information for training and accuracy assessment. Image segmentation should focus on tree crown delineation as opposed to tree stand delineation.

Classification results were poor and did not produce an adequate thematic map of the area in the IKONOS image to distinguish between forest cover types. The IKONOS sensor does not have adequate spatial or spectral resolutions to perform the task at hand. There are published results using IKONOS imagery to classify tree species, but these trees were part of a monoculture where there was little or no mixing within the individual forest stands, or significant amounts of in situ data were collected regarding the species present on the image (Carleer and Wolff, 2004). Use of ancillary data might aid in classification if such data exists. For example, Xu (2007) had success using OBIA to classify forest stands, but this was heavily dependent on the use of elevation data; tree species locations were directly related to elevation changes. Xu also used coarser classification schemes than were used in this study. Also, results may have been improved upon using techniques such as a multitemporal approach, especially if images were collected in different seasons. This would capture changes in phenology and at the very least be able to separate evergreens from their leaf-off deciduous counterparts. Civco et al. (2002)

compared change detection methods using OBIA and hypothesized that classifications based on multitemporal objects could improve results.

Measures of texture were used in an effort to improve classification. While texture measures were used in the feature space to help separate classes, they did not make a significant difference in classification accuracy. Kim et al. (2009) also found that texture measurements did not improve classification results significantly. There are a number of issues in this study that could have influenced the success of texture measures in the image classification, including spatial resolution, kernel size (the *n* x *n* pixel moving window), and the number of classes used (Caridade et al., 2007; Lu et al., 2010). eCognition© uses an object's boundaries to determine kernel size, and summarizes the texture found in each object in order to compare it to other image objects. This is a computationally intense process, since for every pixel of an object a separate pixel matrix has to be calculated (Baatz et al., 2004); the lack of necessary computational power to perform these texture calculations is another limiting factor.

Another approach is to include texture in the segmentation of the image, not just in classification. Texture layers can first be created at the pixel level and then imported into eCognition© along with the individual spectral bands (Kabir et al., 2010; Lu et al., 2010). Conversely, Carleer and Wolff (2006) found that texture classifiers were useful in their non-vegetation classification, but it was spectral characteristics and not texture characteristics that proved most useful in classifying vegetation.

## Conclusion

Object-based image analysis has come a long way since the commencement of this study in 2004. In July 2006, the 1st International Conference on Object-based Image Analysis was held, and the acronyms OBIA and GEOBIA have become part of the remote sensing community's vernacular. OBIA allows for precise and repeatable automation of image segmentation and classification, and will continue to be studied and improved, especially as the resolution of satellite imagery continues to increase. While this study was unable to accurately classify forest stands or delineate individual tree crowns, more is understood about OBIA and future studies using OBIA for forest classification are promising.

## LIST OF REFERENCES


Allen, T.F.H., and T.B. Starr. (1988). Hierarchy: Perspectives for Ecological Complexity University of Chicago Press, Chicago, 328 p.

Allport, S., and D. Howell. (1994). Sermons in Stone: the Stone Walls of New England and New York W.W. Norton & Company, 208 p.

Anderson, J.R., E.E. Hardy, J.T. Roach, and R.E. Whitmer. (1976). A land use and land cover classification system for use with remote sensor data., U.S. Government Printing Office., Washington, D.C.

Baatz, M., and A. Schäpe. (2000). Multi-resolution Segmentation: an optimization approach for high quality multi-scale image segmentation. . *In*: Strobl, J. and T. Blaschke (Eds.), Angewandte Geographische Informationsverarbeitung, Wichmann, Heidelberg, pp. 12-23.

Baatz, M., U.C. Benz, S. Dehghani, M. Heynen, A. Höltje, P. Hofmann, I. Lingenfelder, M. Mimler, M. Sohlbach, M. Weber, and G. Willhauck. (2004). eCognition Professional User Manual 4 Definiens Imaging, München.

Becker, B.L., D.P. Lusch, and J. Qi. (2007). A classification-based assessment of the optimal spectral and spatial resolutions for Great Lakes coastal wetland imagery. *Remote Sensing of Environment* 108(1): 111-120.

Birdsey, R.A., and H.T. Schreuder. (1992). An overview of forest inventory and analysis estimation procedures in the eastern United States – with an emphasis on the components of change. . In: U.S. Department of Agriculture, F.S., Rocky Mountain Forest and Range Experiment Station (Ed.), Fort Collins, CO, pp. 11pp.

Blaschke, T., and G.J. Hay. (2001). Object-oriented image analysis and scale-space: theory and methods for modeling and evaluating multiscale landscape structure. *International Archives of Photogrammetry and Remote Sensing* 34(Part 4/W5): 22-29.

Blaschke, T., and J. Strobl. (2001). What's wrong with pixels? Some recent developments interfacing remote sensing and GIS. *GIS - Zeitschrift für Geoinformationssysteme* 14(6): 12-17.

Blaschke, T., S. Lang, and M.S. Möller. (2005). Object-based analysis of remote sensing data for landscape monitoring: Recent developments. Anais XII Simpósio Brasileiro de Sensoriamento Remoto, Goiania, pp. 2879-2885.

Blaschke, T., and S. Lang. (2006). Object based image analysis for automated information extraction--a synthesis. MAPPS/ASPRS Fall Conference, San Antonio, TX.

Burnett, C., K. Aaviksoo, S. Lang, T. Langanke, and T. Blaschke. (2003). An Object-based Methodology for Mapping Mires Using High Resolution Imagery. Ecohydrological Processes In Northern Wetlands, Tallinn, pp. 6pp.

Burnett, C., and T. Blaschke. (2003). A multi-scale segmentation/object relationship modelling methodology for landscape analysis. *Ecological Modelling* 168(3): 233-249.

Campbell, J.B., and R.H. Wynne. (2011). Introduction to Remote Sensing (5th ed.). Guilford Press.

Caridade, C.M.R., A.R.S. Marcal, and T. Mendonca. (2007). The use of texture for image classification of black & white air photographs. *International Journal of Remote Sensing* 29(2): 593-607.

Carleer, A.P., O. Debeir, and E. Wolff. (2004). Comparison of very high spatial resolution satellite image segmentations. In: Bruzzone, L. (Ed.) Image and Signal Processing for Remote Sensing IX, Bellingham, WA, pp. 532-542.

Carleer, A.P., and E. Wolff. (2004). Exploitation of Very High Resolution Satellite Data for Tree Species Identification. *Photogrammetric Engineering & Remote Sensing* 70(1): 135-140.

Carleer, A.P., O. Debeir, and E. Wolff. (2005). Assessment of Very High Spatial Resolution Satellite Image Segmentations. *Photogrammetric Engineering & Remote Sensing* 7(11): 1285-1294.

Carleer, A.P., and E. Wolff. (2006). Urban land cover multi-level region-based classification of VHR data by selecting relevant features. *International Journal of Remote Sensing* 27(6): 1035-1051.

Chander, G., B.L. Markham, and D.L. Helder. (2009). Summary of current radiometric calibration coefficients for Landsat MSS, TM, ETM+, and EO-1 ALI sensors. *Remote Sensing of Environment* 113: 893-903.

Civco, D.L., J.D. Hurd, E.H. Wilson, M. Song, and Z. Zhang. (2002). A comparison of land use and land cover change detection methods. ASPRS-ACSM Annual Conference and FIG XXII Congress.

Cleve, C., M. Kelly, F.R. Kearns, and M. Moritz. (2008). Classification of the wildland-urban interface: A comparison of pixel- and object-based classifications using high-resolution aerial photography. *Computers, Environment and Urban Systems* 32(4): 317-326.

Coe, S., M. Alberti, J.A. Hepinstall, and R. Coburn. (2005). A hybrid approach to detecting impervious surface at multiple scales. Proceedings of the ISPRS WG VII/1 "Human Settlements and Impact Analysis" 3rd International Symposium Remote Sensing and Data Fusion Over Urban Areas (URBAN 2005) and 5th International Symposium Remote Sensing of Urban Areas (URS 2005), Tempe, AZ.

Cohen, J. (1960). A coefficient of agreement for nominal scales. *Educational and Psychological Measurement* 20(1): 37-40.

Congalton, R.G., R.G. Oderwald, and R.A. Mead. (1983). Assessing Landsat classification accuracy using discrete multivariate statistical techniques. *Photogrammetric Engineering & Remote Sensing* 49(12): 1671-1678.

Congalton, R.G. (1991). A review of assessing the accuracy of classifications of remotely sensed data. *Remote Sensing of Environment* 37: 35-46.

Congalton, R.G., and K. Green. (1999). Assessing the Accuracy of Remotely Sensed Data: Principles and Practices Lewis Publishers, Boca Raton, 137 p.

Congalton, R.G., and K. Green. (2009). Assessing the Accuracy of Remotely Sensed Data: Principles and Practices (2nd ed.). CRC Press, Boca Raton, 183 p.

D'Eon, R.G., and D. Delparte. (2005). Effects of radio-collar position and orientation on GPS radio-collar performance, and the implications of PDOP in data screening. *Journal of Applied Ecology* 42(2): 383-388.

Dean, A.M., and G.M. Smith. (2003). An evaluation of per-parcel land cover mapping using maximum likelihood class probabilities. *International Journal of Remote Sensing* 24(14): 2905-2920.

Desclée, B., P. Bogaert, and P. Defourny. (2006). Forest change detection by statistical object-based method. *Remote Sensing of Environment* 102(1–2): 1-11.

Dial, G., L. Gibson, and R. Poulsen. (2001). IKONOS satellite imagery and its use in automated road extraction. *In*: Baltsavias, E.P., A. Gruen and L. Van Gool (Eds.), Automatic Extraction of Man-Made Objects from Aerial and Space Images (III), Taylor & Francis, Zürich, pp. 357-367.

DiGregorio, A., and L.J.M. Janse. (1998). Land Cover Classification System (LCCS): Classification Concepts and User Manual. Environment and Natural Resources Service, GCP/RAF/287/ITA Africover - East Africa Project and Soil Resources, Management and Conservation Service. FAO, Rome, pp. 157.

Doraiswamy, P.C., J.L. Hatfield, T.J. Jackson, B. Akhmedov, J. Prueger, and A. Stern. (2004). Crop condition and yield simulations using Landsat and MODIS. *Remote Sensing of Environment* 92(4): 548-559.

Durrieu, S., T. Tormos, P. Kosuth, and C. Golden. (2007). Influence of training sampling protocol and of feature space optimization methods on supervised classification results. Geoscience and Remote Sensing Symposium, 2007. IGARSS 2007. IEEE International, pp. 2030-2033.

Ekercin, S. (2007). Water Quality Retrievals from High Resolution Ikonos Multispectral Imagery: A Case Study in Istanbul, Turkey. *Water, Air, & Soil Pollution* 183(1): 239-251.

Eyre, F.H. Ed.^Eds. (1980). Forest Cover Types of the United States and Canada, Society of American Foresters, Washington, D.C.

Farina, A. (2000). Landscape Ecology in Action Kluwer Academic Publishers, Dordrecht, 412 p.

Farina, A. (2006). Principles and Methods in Landscape Ecology: Toward a Science of Landscape Springer, Dordrecht.

Ferro, C.J.S. (1998). Scale and Texture in Digital Image Classification. Eberly College of Arts and Sciences, West Virginia University, Morgantown, WV, pp. 60.

Flanders, D., M. Hall-Beyer, and J. Pereverzoff. (2003). Preliminary evaluation of eCognition object-based software for cut block delineation and feature extraction. *Canadian Journal of Remote Sensing* 29(4): 441-452.

Foody, G.M. (1999). The Continuum of Classification Fuzziness in Thematic Mapping. *Photogrammetric Engineering & Remote Sensing* 65(4): 443-451.

Foody, G.M. (2002). Status of land cover classification accuracy assessment. *Remote Sensing of Environment* 80: 185-201.

Foster, D.R. (1992). Land-Use History (1730-1990) and Vegetation Dynamics in Central New England, USA. *Journal of Ecology* 80(4): 753-771.

Foster, D.R., and J.D. Aber. (2006). Forests in Time: The Environmental Consequences of 1,000 Years of Change in New England Yale University Press, 496 p.

Frauman, E., and E. Wolff. (2005). Segmentation of very high spatial resolution satellite images in urban areas for segments-based classification. Proc. International Symposium of Remote Sensing and Data Fusion Over Urban Areas, 5th International Symposium of Remote Sensing of Urban Areas, Tempe, AZ.

Grenier, M., S. Labrecque, M. Benoit, and M. Allard. (2008). Accuracy Assessment Method for Wetland Object-Based Classification. Proceedings of GEOBIA 2008-- Pixels, Objects, Intelligence: Geographic Object-Based Image Analysis for the 21st Century, Calgary, Alberta.

Hagen, S. (2010). IKONOS Top of Atmosphere Correction for Normalized Difference Vegetation Index (NDVI). Applied Geosolutions, LLC, Newmarket, NH.

Hansen, M.C., D.P. Roy, E. Lindquist, B. Adusei, C.O. Justice, and A. Altstatt. (2008). A method for integrating MODIS and Landsat data for systematic monitoring of forest cover and change in the Congo Basin. *Remote Sensing of Environment* 112(5): 2495-2513.

Haralick, R.M., K. Shanmugam, and I.h. Dinstein. (1973). Textural Features for Image Classification. *IEEE Transactions on Systems, Man, and Cybernetics* SMC-3(6): 610-621.

Haralick, R.M. (1979). Statistical and Structural Approaches to Texture. *Proceedings of the IEEE* 67(5): 786-808.

Heath, B.L. (2008). Evaluating scale to achieve optimal image classification accuracy in New Hampshire forests. Department of Natural Resources, University of New Hampshire, Durham, pp. 128.

Husch, B. (1971). Planning a forest inventory Food & Agriculture Organization, Rome, 120 p.

Jensen, J.R. (2005). Introductory Digital Image Processing: A Remote Sensing Perspective (3rd ed.). Prentice-Hall, Upper Saddle River, 526 p.

Jobin, B., S. Labrecque, M. Grenier, and G. Falardeau. (2008). Object-Based Classification as an Alternative Approach to the Traditional Pixel-Based Classification to Identify Potential Habitat of the Grasshopper Sparrow. *Environmental Management* 41(1): 20-31.

Kabir, S., D.-C. He, M.A. Sanusi, and W.M.A. Wan Hussin. (2010). Texture analysis of IKONOS satellite imagery for urban land use and land cover classification. *Imaging Science Journal* 58: 163-170.

Key, T., T.A. Warner, J.B. McGraw, and M.A. Fajvan. (2001). A Comparison of Multispectral and Multitemporal Information in High Spatial Resolution Imagery for Classification of Individual Tree Species in a Temperate Hardwood Forest. *Remote Sensing of Environment* 75(1): 100-112.

Kim, M., M. Madden, and T. Warner. (2008). Estimation of optimal image object size for the segmentation of forest stands with multispectral IKONOS imagery. *In*: Blaschke, T., S. Lang and G.J. Hay (Eds.), Object-Based Image Analysis, Springer Berlin Heidelberg, pp. 291-307.

Kim, M., M. Madden, and T.A. Warner. (2009). Forest type mapping using object-specific texture measures from multispectral Ikonos imagery: segmentation quality and image classification issues. *Photogrammetric Engineering and Remote Sensing* 75(7): 819-829.

Klemas, V.V., J.E. Dobson, R.L. Ferguson, and K.D. Haddad. (1993). A Coastal Land Cover Classification System for the NOAA Coastwatch Change Analysis Project. *Journal of Coastal Research* 9(3): 862-872.

Larrañaga, A., J. Álvarez-Mozos, and L. Albizua. (2011). Crop classification in rain-fed and irrigated agricultural areas using Landsat TM and ALOS/PALSAR data. *Canadian Journal of Remote Sensing* 37(1): 157-170.

Leduc, F. (2004). Feature space optimization prior to fuzzy image classification. In: Svensson, P. and J. Schubert (Eds.), 7th International Conference on Information Fusion, International Society of Information Fusion, Stockholm, Sweden, pp. 547-554.

Lennartz, S.P. (2004). Pixel- versus segment-based image processing techniques for forest cover type mapping using IKONOS imagery. Department of Natural Resources, University of New Hampshire, Durham, pp. 79.

Land Processes Distributed Active Archive Center (LPDAAC) (2011). MODIS Overview.

Lu, D., S. Hetrick, and E. Moran. (2010). Land Cover Classification in a Complex Urban-Rural Landscape with QuickBird Imagery. *Photogrammetric Engineering & Remote Sensing* 76(10): 1159-1168.

Martin, M.E., S.D. Newman, J.D. Aber, and R.G. Congalton. (1998). Determining Forest Species Composition Using High Spectral Resolution Remote Sensing Data. *Remote Sensing of Environment* 65(3): 249-254.

Myint, S.W., P. Gober, A. Brazel, S. Grossman-Clarke, and Q. Weng. (2011). Per-pixel vs. object-based classification of urban land cover extraction using high spatial resolution imagery. *Remote Sensing of Environment* 115(5): 1145-1161.

National Weather Service. (2011). Climate Data: 30 Year Normals 1981-2010.

Núñez, J., X. Otazu, O. Fors, A. Prades, V. Palà, and R. Arbiol. (1999). Multiresolution-Based Image Fusion with Additive Wavelet Decomposition. *IEEE Transactions on Geoscience & Remote Sensing* 37(3): 8p.

Ouma, Y.O., J. Tetuko, and R. Tateishi. (2008). Analysis of co-occurrence and discrete wavelet transform textures for differentiation of forest and non-forest vegetation in very-high-resolution optical-sensor imagery. *International Journal of Remote Sensing* 29(12): 3417-3456.

Paul, F., C. Huggel, and A. Kääb. (2004). Combining satellite multispectral image data and a digital elevation model for mapping debris-covered glaciers. *Remote Sensing of Environment* 89(4): 510-518.

Philipp-Foliguet, S., and L. Guigues. (2008). Multi-scale criteria for the evaluation of image segmentation algoritms. *Journal of Multimedia* 3(5): 42-56.

Platt, R.V., and L. Rapoza. (2008). An Evaluation of an Object-Oriented Paradigm for Land Use/ Land Cover Classification. *The Professional Geographer* 60(1): 87-100.

Plourde, L.C. (2000). Important Factors in Assessing the Accuracy of Remotely Sensed Forest Vegetation Maps: A Comparison of Sampling and Total Enumeration and Their Effects on Data Accuracy. Department of Natural Resources, University of New Hampshire, Durham, pp. 221.

Plourde, L.C. (2007). Estimating species abundance in a northern temperate forest using spectral mixture analysis. *Photographic Engineering & Remote Sensing* 73(7): 829-840.

Pugh, S.A. (1997). Applying spatial autocorrelation analysis to evaluate error in New England forest cover type maps derived from Landsat Thematic Mapper data. Forest Resources, University of New Hampshire, Durham.

Radoux, J., P. Bogaert, D. Fasbender, and P. Defourny. (2011). Thematic accuracy assessment of geographic object-based image classification. *International Journal of Geographical Information Science* 25(6): 895-911.

Röder, A., J. Hill, B. Duguy, J.A. Alloza, and R. Vallejo. (2008). Using long time series of Landsat data to monitor fire events and post-fire dynamics and identify driving factors. A case study in the Ayora region (eastern Spain). *Remote Sensing of Environment* 112(1): 259-273.

Soares, J.V., C.D. Rennó, A.R. Formaggio, C.d.C.F. Yanasse, and A.C. Frery. (1997). An Investigation of the Selection of Texture Features for Crop Discrimination Using SAR Imagery. *Remote Sensing of Environment* 59: 234-247.

Stefanov, W.L., M.S. Ramsey, and P.R. Christensen. (2001). Monitoring urban land cover change: An expert system approach to land cover classification of semiarid to arid urban centers. *Remote Sensing of Environment* 77(2): 173-185.

Stehman, S.V., and R.L. Czaplewski. (1998). Design and Analysis for Thematic Map Accuracy Assessment: Fundamental Principles. *Remote Sensing of Environment* 64(3): 331-344.

Story, M., and R. Congalton. (1986). Accuracy assessment - A user's perspective. *Photogrammetric Engineering and Remote Sensing* 52(3): 397-399.

Thenkabail, P.S. (2004). Inter-sensor relationships betwen IKONOS and Landsat-7 ETM+ NDVI data in three ecoregions of Africa. *International Journal of Remote Sensing* 25(2): 389-408.

Townshend, J.R.G., C. Huang, S.N.V. Kalluri, R.S. Defries, S. Liang, and K. Yang. (2000). Beware of per-pixel characterization of land cover. *International Journal of Remote Sensing* 21(4): 839 - 843.

Tucker, C.J. (1979). Red and photographic infrared linear combinations for monitoring vegetation. *Remote Sensing of Environment* 8(2): 127-150.

Turner, M.G., R.H. Gardner, and R.V. O'Neill. (2001). Landscape Ecology in Theory and Practice: Pattern and Process Springer Science, New York.

USFS, Northeastern Research Station. (2002). The Granite State's Forests: Trends in the Resource. United States Department of Agriculture, Forest Service, Northeastern Research Station, NE-INF-141-02, pp. 9.

Van Delm, A., and H. Gulinck. (2011). Classification and quantification of green in the expanding urban and semi-urban complex: Application of detailed field data and IKONOS-imagery. *Ecological Indicators* 11(1): 52-60.

van der Sande, C.J., S.M. de Jong, and A.P.J. de Roo. (2003). A segmentation and classification approach of IKONOS-2 imagery for land cover mapping to assist flood risk and flood damage assessment. *International Journal of Applied Earth Observation and Geoinformation* 4(3): 217-229.

Whiteside, T., G. Boggs, and S. Maier. (2010). Area-based validity assessment of single- and multi-class object-based image analysis. 15th Australasian Remote Sensing and Photogrammetry Conference, Alice Spings.

Wu, J. (1999). Hierarchy and Scaling: Extrapolating Information Along a Scaling Ladder. *Canadian Journal of Remote Sensing* 25(4): 367-380.

Xu, B. (2007). Object-based image analysis (OBIA) of vegetation in Great Smoky Mountains National Park. Department of Geography, University of Georgia, Athens, pp. 89.

Yan, G., J.F. Mas, B.H.P. Maathuis, Z. Xiangmin, and P.M. Van Dijk. (2006). Comparison of pixel-based and object-oriented image classification approaches—a case study in a coal fire area, Wuda, Inner Mongolia, China. *International Journal of Remote Sensing* 27(18): 4039-4055.

Zhu, C., and X. Yang. (1998). Study of remote sensing image texture analysis and classification using wavelet. *International Journal of Remote Sensing* 19(16): 3197-3203.

# APPENDICES

**APPENDIX A**

Modified classification scheme used for forest classification (Eyre, 1980)

<u>Schema definitions used for determinate and fuzzy 'Forest stand' classification and accuracy assessment</u>

NOTE: *The MMU for 'Forest stand' objects was 30m$^2$. Each object must be at least 30% forested to be considered a useable sample.*

WP: Eastern white pine (*Pinus strobus*) comprises 70% or more of the stand

HE: Eastern hemlock (*Tsuga canadensis*) comprises 70% or more of the stand

WH: Eastern white pine and eastern hemlock together comprise a majority of the stand, and each represent at least 25% of the total. Neither species alone comprises more than 50% of the total

BH: American beech (*Fagus grandifolia*) comprises at least 30% of the forest cover type. Eastern white pine and/or eastern hemlock comprise less than 50% of the forest cover type

RM: Red maple (*Acer rubrum*), sugar maple (*Acer saccharum*), or some combination of the two, represent 50% or more of the forest stand

OAK: White oak (*Quercus alba*), black oak (*Quercus velutina*), and/or northern red oak (*Quercus rubra*) comprise at least 50% of the stocking. Eastern white pine and/or eastern hemlock comprise less than 50% of the forest cover type

MX: At least two or more deciduous species combined (besides *Quercus spp.*) represent 30% or more of the forested area

OF: Any mix of coniferous and/or deciduous species not represented in one of the above categories

NF: Any other vegetated cover type (forest within permanent or semi-permanent standing water, agriculture, pasture, shrubland, etc)

NOTE: *Preference is given to deciduous species in the following order for the BEST position (most preferred to least preferred): 1. Oak, 2. Maple, 3. Beech, 4. Birch. There is no particular order for species/categories in the ACCEPTABLE positions*

1. Is the stand 70% Hemlock?
   YES, go to question 2
   NO, go to question 3

2. Is the stand >=20% Pine?
   YES, classified as [Hem, Pine]
   NO, go to question 4

3. Is the stand 70% Pine?
   YES, go to question 5
   NO, go to question 6

4. Is the stand 30% of a <u>single</u> deciduous species?
   YES, classified as [Hem, DE]
   NO, classified as [Hem]

5. Is the stand >=20% Hemlock?
   YES, classified as [Pine, Hem]
   NO, go to question 7

6. Is the stand 30% Pine?
   YES, go to question 8
   NO, go to question 9

7. Is the stand 30% of a <u>single</u> deciduous species?
   YES, classified as [Pine, DE]
   NO, classified as [Pine]

8. Is the stand at least 30% Hemlock?
   YES, go to question 10
   NO, go to question 11

9. Is the stand 30% Hemlock?
   YES, go to question 13
   NO, go to question 14

10. Is the stand at least 30% of a <u>single</u> deciduous species?
    YES, classified as [Pine, Hem, DE]
    NO, classified as [Pine, Hem]

11. Is the stand at least 30% of any other species?
    YES, go to question 12
    NO, go to question 41

12. –
    a. If the stand is =30% of any deciduous species, classified as [Pine, DE1, DE2]
    b. If the stand is >30% of a <u>single</u> deciduous species but comprises less or equal to the same area as the Pine, classified as [Pine, DE]
    c. If the stand is >30% of a <u>single</u> deciduous species and comprises more area than the Pine, classified as [DE, Pine]

13. Is the stand at least 30% of any deciduous species?
    YES, go to question 15
    NO, go to question 42

14. Is the stand 70% of a <u>single</u> deciduous species?
    YES, classified as [DE]
    NO, go to question 16

15. –
    a. If the stand is =30% of any deciduous species, classified as [Hem, DE1, DE2]
    b. If the stand is >30% of a <u>single</u> deciduous species but comprises less than or equal to the same area as the Hemlock, classified as [Hem, DE]
    c. If the stand is >30% of a <u>single</u> deciduous species and comprises more area than the Hemlock, classified as [DE, Hem]

16. Is the stand at least 50% of a <u>single</u> deciduous species?
    YES, go to question 17
    NO, go to question 18

17. Is the stand at least 30% of a second deciduous species?
    YES, classified as [DE1, DE2] *<u>if 50/50, place the more preferred of the species in DE1</u>*
    NO, go to question 19

18. Is the stand at least 30% Oak?
    YES, go to question 20
    NO, go to question 21

19. Is the stand =20% Pine and =20% Hemlock?
    YES, classified as [DE, Pine, Hem]
    NO, go to question 32

20. Is the stand at least 30% of any other deciduous species?
    YES, go to question 29
    NO, go to question 30

21. Is the stand = 30% of any two or more deciduous species besides Oak?
    YES, classified as [DE1, DE2, DE3] *<u>if equal in area, place the more preferred of the species in DE1</u>*
    NO, go to question 22

22. Is the stand at least 40% of a <u>single</u> deciduous species?
    YES, go to question 23
    NO, go to question 24

23. Is the stand at least 30% of a second deciduous species?
    YES, go to question 25
    NO, go to question 26

24. Is the stand at least 40% of a non-forested feature, such as pasture, shrubland, water, or development?
    YES, classified as [NF]
    NO, this point is not an acceptable GCP, should not be used in classification

25. Is the stand =20% of Pine or Hemlock?
    YES, classified as [DE40, DE30, Pine or Hem]
    NO, classified as [DE40, DE30]

26. Is the stand =20% of Pine and =20% Hemlock?
    YES, classified as [DE, Pine, Hem]
    NO, go to question 27

27. Is the stand =20% of Pine or Hemlock?
    YES, classified as [DE, *Pine* or *Hem*]
    NO, go to question 28

28. Is the stand at least 20% of a non-forested feature, such as pasture, shrubland, water, or development?
    YES, classified as [DE, NF]
    NO, classified as [DE]

29. Is the stand at least 30% of a non-forested feature, such as pasture, shrubland, water, or development?
    YES, classified as [Oak, DE2, NF]
    NO, go to question 31

30. Is the stand = 50% of a non-forested feature, such as pasture, shrubland, water, or development?
    YES, go to question 36
    NO, go to question 37

31. Is the stand =20% of Pine and =20% Hemlock?
    YES, classified as [Oak, DE2, Pine, Hem]
    NO, go to question 35

32. Is the stand =20% Pine or Hemlock?
    YES, go to question 33
    NO, go to question 34

33. Is the stand at least 20% of a non-forested feature, such as pasture, shrubland, water, or development?
    YES, classified as [DE, *Pine* or *Hem*, NF]
    NO, classified as [DE, *Pine* or *Hem*]

34. Is the stand = 30% of a non-forested feature, such as pasture, shrubland, water, or development?
    YES, classified as [DE, NF]
    NO, classified as [DE]

35. Is the stand =20% of Pine or Hemlock?
    YES, classified as [Oak, DE2, *Pine* or *Hem*]
    NO, classified as [Oak, DE2, DE3]

36. Is the stand =20% of Pine or Hemlock?
    YES, classified as [NF, Oak, *Pine* or *Hem*]
    NO, classified as [NF, Oak]

37. Is the stand = 30% of a non-forested feature, such as pasture, shrubland, water, or development?
    YES, go to question 38
    NO, go to question 39

38. Is the stand =20% of Pine or Hemlock?
    YES, classified as [Oak, NF, *Pine* or *Hem*]
    NO, classified as [Oak, NF]

39. Is the stand =20% Pine and =20% Hem?
    YES, classified as [Oak, Pine, Hem]
    NO, go to question 40

40. Is the stand =20% Pine or Hem?
    YES, classified as [Oak, Pine or Hem]
    NO, classified as [NF]

41. Is the stand =40% of a non-forested feature, such as pasture, shrubland, water, or development?
    YES, classified as [NF, Pine]
    NO, classified as [Pine]

42. Is the stand =40% of a non-forested feature, such as pasture, shrubland, water, or development?
    YES, classified as [NF, Hem]
    NO, classified as [Hem]

**APPENDIX B**

Object features used in the Feature Space Optimizer (FSO) to find features for classification

1. Layer values
    a. Mean
        i. Blue Band
        ii. Green Band
        iii. Red Band
        iv. NIR Band
        v. Pan Band
        vi. PCA Band
        vii. NDVI Band
        viii. EVI Band
        ix. NIR/Red Band
    b. Standard Deviation
        i. Blue Band
        ii. Green Band
        iii. Red Band
        iv. NIR Band
        v. Pan Band
        vi. PCA Band
        vii. NDVI Band
        viii. EVI Band
        ix. NIR/Red Band
    c. Brightness
    d. Max Difference
2. Shape
    a. Area
    b. Border index
    c. Compactness
    d. Compactness (polygon)
    e. Density
    f. Shape Index
    g. Length/Width
    h. Elliptic Fit
    i. Length/Width (only main line)
    j. Asymmetry
    k. Main direction
    l. Radius of largest enclosed ellipse
    m. Radius of smallest enclosing ellipse
    n. Rectangular Fit
    o. Roundness
3. Texture
    a. GLCM Entropy Pan (all directions)

b. GLCM Homogeneity Pan (all directions)
c. GLCM Contrast Pan (all directions)
d. GLCM Dissimilarity Pan (all directions)
e. GLCM Angular 2nd moment Pan (all directions)
f. GLCM Correlation Pan (all directions)

**APPENDIX C**

Equations to measure texture and their definitions
(Haralick et al., 1973; Soares et al., 1997; Ouma et al., 2008)

I = entire image
$N_x$ = cells in the *x* direction
$L_x$ = all of the cells in the x direction – (1,2,..., $N_x$)
$N_y$ = cells in the *y* direction
$L_y$ = all of the cells in the *y*-direction – (1,2,..., $N_y$)
$N_g$ = gray level in a cell
G = number of gray levels in the image– (1,2,...,$N_g$)
$P_{i,j}$ = the relative frequency with which a pixel pair separated by a distance (*d*) occur on the image, one with gray tone *i* and the other with gray tone *j*
R = number of occurrences of a particular neighboring resolution cell pair (aka unique cell pair) (normalizing constant)
$R_H$, $R_V$, $R_{RD}$, $R_{LD}$ = number of neighboring resolution cell pairs in the horizontal, vertical, right diagonal, or left diagonal direction
μ = mean
σ = standard deviation

---

*Homogeneity*: a measure of the lack of variability in gray levels; in a homogeneous image, there are very few dominant gray tone transitions; inversely correlated with contrast

$$HOM = \sum_{i=0}^{N-1} \sum_{j=0}^{N-1} \frac{P_{i,j}}{1+(i-j)^2} \tag{10}$$

*Angular Second Moment*: measure of uniformity; measures pixel pair repetition; similar to homogeneity

$$ASM = \sum_{i=0}^{N-1} \sum_{j=0}^{N-1} P_{i,j}^2 \tag{11}$$

*Contrast*: measure of the amount of local variation present; measures the degree of difference in gray levels; inversely correlated with homogeneity

$$CON = \sum_{i=0}^{N-1} \sum_{j=0}^{N-1} P_{i,j}\,(i-j)^2 \tag{12}$$

*Dissimilarity*: similar to contrast, except that values increase linearly as values move away from the major diagonal, not exponentially as is the case with contrast

$$DIS = \sum_{i=0}^{N-1} \sum_{j=0}^{N-1} P_{i,j} \, |i - j| \tag{13}$$

*Entropy*: a measure of disorder or lack of uniformity; high entropy indicates heterogeneous or completely random pixels; inversely correlated to angular 2nd moment

$$ENT = \sum_{i=0}^{N-1} \sum_{j=0}^{N-1} - P_{i,j} \ln P_{i,j} \tag{14}$$

*Correlation*: a measure of gray-tone linear dependencies on an image; high correlation values indicate linear relationships between pixels

$$COR = \sum_{i=0}^{N-1} \sum_{j=0}^{N-1} \frac{(i - \mu_I)(j - \mu_J)}{\sigma_I \, \sigma_J} \tag{15}$$